NACA RM E56F26

NACA

RESEARCH MEMORANDUM

EXPERIMENTAL INVESTIGATION OF DIFFUSER PRESSURE-RATIO CONTROL WITH SHOCK-POSITIONING LIMIT ON 28-INCH RAM-JET ENGINE

By William R. Dunbar, Carl B. Wentworth, and Robert J. Crowl

Lewis Flight Propulsion Laboratory
Cleveland, Ohio

NATIONAL ADVISORY COMMITTEE
FOR AERONAUTICS

WASHINGTON

January 15, 1957

NATIONAL ADVISORY COMMITTEE FOR AERONAUTICS

RESEARCH MEMORANDUM

EXPERIMENTAL INVESTIGATION OF DIFFUSER PRESSURE-RATIO CONTROL WITH SHOCK-POSITIONING LIMIT ON 28-INCH RAM-JET ENGINE

By William R. Dunbar, Carl B. Wentworth, and Robert J. Crowl

SUMMARY

The performance of a diffuser static-pressure-ratio control with a normal shock-positioning limit was investigated on a 28-inch ram-jet engine installed in an altitude free-jet facility. The investigation was conducted at free-stream Mach numbers of 2.35 and 2.50, altitudes of 50,000, 60,000, and 65,000 feet, and angles of attack of 0 and $\pm 7^{\circ}$.

The basic pressure-ratio control set the ratio of a diffuser static pressure to a diffuser cone-surface static pressure at any desired level within the engine operating range. By using this pressure ratio, the operation of the control was independent of altitude. The cone surface, or reference pressure, provided compensation, to a limited extent, for variations in Mach number. The shock-positioning limit loop utilized the static pressure on the diffuser innerbody in the plane of the cowl lip to permit operation near maximum diffuser recovery and to protect against blowout at angle of attack.

The results obtained indicate that the control was capable of successful operation over the range of engine and flight conditions tested. Minimum response times approaching the system dead time were obtained with small amounts of overshoot, and the control successfully recovered from disturbances which placed the engine well beyond the steady-state blowout limits. The basic pressure-ratio control was primarily affected by variations in engine gain which prevented optimum performance at all conditions with fixed control settings.

The shock-positioning limit effectively reduced response times for disturbances which resulted in subcritical operation and permitted safe operation of the engine at nearly maximum recovery. Operation of the limit at a $+7^{\circ}$ angle of attack required limit gains in excess of those allowable for stable continuous limit operation at zero angle of attack. However, it appeared feasible to stabilize the limit loop by addition of a first-order lag without seriously impairing the normal operation of the limit.

INTRODUCTION

Most of the work at the NACA Lewis laboratory on ram-jet engine controls (refs. 1 to 6) has dealt with control techniques designed to maintain a particular mode of engine operation. These techniques include such controls as optimalizer and shock-positioning systems designed to maintain peak engine performance, and others, such as diffuser pressure-ratio and normal shock-positioning systems, designed to maintain a specific level of operation at some value less than peak.

The emphasis in most of these previous control investigations has been on the ability of the control to meet the requirements of a nonmaneuvering, strategic type of missile. That is, the accuracy with which the desired operation may be maintained and the proximity to peak performance which could be achieved were of prime consideration.

Contrasted with the requirements of the strategic missile are those of an interceptor-type missile or piloted vehicle in which any thrust level within the engine capabilities may be desired. In addition, the control system must be expected to perform satisfactorily over a range of altitudes and Mach numbers and in the presence of maneuvers resulting in large variations in angle of attack and yaw.

One of the control techniques previously mentioned, that of diffuser pressure-ratio control, is adaptable to variable thrust applications, providing a suitable limit is incorporated to prevent continued subcritical operation.

In order to provide information on such a control system, an investigation was undertaken of a diffuser pressure-ratio control with a shock-positioning limit. The objectives of this investigation were (1) to determine optimum control constants for the basic pressure-ratio control; (2) to investigate the problems associated with incorporating the shock-positioning limit and its effect on system performance; and (3) to investigate the effects on system performance of changes in engine operating point and flight conditions, in particular the problems connected with angle-of-attack operation.

This report includes a description of the characteristics, both static and dynamic, of all components of the two control loops of the control system; the response and stability characteristics of the control system as a function of control constants, engine operating conditions, and flight conditions; and a discussion of control limitations and possible improvements.

APPARATUS AND INSTRUMENTATION

The apparatus and instrumentation used in this investigation consisted of a 28-inch ram-jet engine installed in an altitude free-jet

facility, an electrohydraulic fuel servo system, steady-state and transient instrumentation for measurement of engine pressures, oscillograph recorders on which the transient data were recorded, and an electronic analog computer which provided the necessary control functions.

Engine and Facility

The altitude free-jet facility with the engine installed is shown in figure 1. The engine inlet is submerged in an air jet issuing from the supersonic nozzle. Two interchangeable nozzles provided free-stream Mach numbers of 2.35 and 2.50. The nozzles could be rotated about a horizontal pivot to provide simulation of angles of attack from $+7^{\circ}$ to -7°. The inlet air was heated to appropriate temperatures by gas-fired heat exchangers. The pressure in the compartment containing the engine was low enough to ensure choked flow in the exhaust nozzle at all conditions.

The engine is shown in greater detail in figure 2. (All symbols are defined in appendix A.) The combustion-chamber diameter at its largest section was 28 inches. The actual internal-flow-area variation throughout the engine is shown in figure 3. The grid, located at station 57, is designed to improve the air flow profile prior to injection of fuel at station 60. The exhaust nozzle had a minimum area of 0.70 times the combustion-chamber area. The diffuser inlet had a single-shock 25° half-angle, conical spike and was designed to have the conical shock wave at the cowl lip at Mach 2.50.

The engine fuel-injection system was comprised of two independent fuel manifolds equipped with spring-loaded, variable-area nozzles. One manifold, designated the inner ring, was supplied with fuel equivalent to an over-all fuel-air ratio of 0.037 throughout the investigation. The other manifold, designated the outer ring, was used in the control system to supply the desired fuel flow in excess of the lean-limit level set with the inner ring.

In general, the response of diffuser static pressures downstream of the normal shock to fuel flow will be similar to the frequency-response characteristics shown in figure 4. The dynamic characteristics of the engine are reported in detail in reference 7.

Fuel System

The fuel system used in the control consisted of the outer-ring manifold and nozzles of the engine, an electrohydraulic fuel servo system, and the associated piping.

The fuel control contained an electrohydraulic servo system which positioned a throttle in a specially designed fuel-metering valve in response to an input-voltage signal. The fuel-metering valve incorporated a differential relief valve, which maintained a constant pressure drop across the metering orifice. Since the metering area was a linear function of throttle position, the fuel flow at the valve was also a linear function of throttle position and of input voltage to the fuel servo. This type of throttle-plus-reducing-valve, differential-pressure regulator system is described in detail in reference 8.

The actual flow from the fuel-injection nozzles could not be readily measured dynamically. However, a theoretical analysis with experimental verification indicated that the manifold pressure drop P_o was indicative of actual nozzle fuel flow within ± 5 percent to approximately 40 cps with approximately 30° error in phase at 40 cps. Therefore, for the frequencies of principal interest in the controls investigation (less than 20 cps), the manifold pressure drop P_o may be considered dynamically the same as the nozzle fuel flow $w_{f,o}$.

The frequency-response characteristics of the complete fuel system are shown in figure 5. The peak in the amplitude characteristic at 25 cps is due to a resonance of the manifold and connected piping.

The manifold pressure drop was measured with differential-pressure transducers connected to the fuel manifold and referenced to the static engine pressure in the region of the manifolds. The frequency response of the pickups and connected tubing was essentially flat to at least 100 cps with less than $\pm 10^\circ$ phase shift.

The fuel control panel and associated equipment are shown in rack 1 of figure 6. Steady-state fuel flow was measured with turbine-type flowmeters.

Instrumentation

Engine gas pressures. - For transient measurement of engine pressures, reluctance-type pressure transducers were used. The frequency-response characteristics of the pickups and associated tubing are shown in figure 7. In addition to using the transducers for transient measurement of pressures, the static engine characteristics were obtained by plotting engine pressures directly as a function of fuel flow on an X-Y recorder, shown in rack 2 of figure 6.

Manometers were used for normal steady-state pressure measurements and calibration of transient pickups.

Angle of attack. - Angle of attack was determined by means of calibrated physical stops on the supersonic-nozzle actuator mechanism.

Recording equipment. - All transients were recorded on sensitized paper with oscillographs using galvanometers with natural frequencies of 200 to 500 cps. The recording apparatus, including the carrier-type amplifiers and recorders, are shown in rack 3 of figure 6. In addition, certain variables of particular interest were also recorded on a direct-inking oscillograph with a frequency response of 100 cps. This oscillograph may be seen in rack 5, figure 6.

5043

Computer

The necessary computation for control purposes was performed by an electronic differential analyzer, which is shown in rack 4, figure 6. The computer performs the required operations through the use of high-gain d-c operational amplifiers and associated plug-in input and feedback impedances.

DESCRIPTION OF CONTROL

Control Action

The control system investigated consisted of a basic control loop and a limit loop. The basic loop held the ratio of a diffuser static pressure to a reference pressure at any desired value, which provides operation independent of altitude. This ratio is maintained in the control by holding the control pressure equal to the reference pressure times the desired pressure ratio. The advantage of this method is that it makes it unnecessary to divide the two pressure signals in the control.

A simplified block diagram of this basic control system is shown in figure 8(a). The basic control and the reference pressures are converted to equivalent voltages by means of the sensors and amplifiers. The reference-pressure signal is then multiplied by the desired pressure ratio and becomes the reference input, which is equal to the set value of the basic control pressure. The difference between the reference input and the actual value of the basic control signal is the control error signal, which goes to the control containing proportional-plus-integral control action. The control output actuates the fuel servo and varies the outer-ring fuel flow as required to bring the error signal to zero.

By varying the desired pressure ratio, the basic control may be used to vary the engine thrust over the allowable range. The minimum level in this system was determined by the fuel-air ratio set with the inner-ring fuel flow. The maximum level of operation is determined by the diffuser static-pressure-ratio characteristic, which, in general,

increases to a peak value corresponding to critical diffuser operation and then decreases for subcritical operation. Obviously, if a desired pressure ratio greater than the peak value is called for, the control will continuously increase the fuel flow and drive the engine further and further subcritical until the blowout limit is reached. In addition, attempting to set exactly the peak pressure ratio is inherently unstable, since any disturbance which causes even temporary subcritical operation will result in a lower actual pressure ratio than the set value and will cause the control to increase fuel flow, resulting in blowout, as described before.

In actual practice there will be a range of supercritical pressure ratios, just below peak, that are not safe to set with the control, as just described, since momentary subcritical operation can result in the same or lower pressure ratios and the subsequent instability described. Therefore, in order to allow operation as close to peak as possible, it is necessary to utilize some form of limit to prevent continued subcritical operation.

The limit used senses the position of the normal shock by measurement of the static-pressure rise on the innerbody in the plane of the cowl lip as the shock is expelled. This limit pressure is converted to an equivalent voltage by means of a sensor and amplifier, as shown in figure 8(b), and then goes into the limit control, which provides a bias to reduce the limit signal to zero for supercritical operation and also provides a variable gain. The resulting limit signal is then combined with the basic control at the summing point. For a balanced condition, the error signal must be zero and, therefore, the reference signal minus the basic control signal minus the limit signal must equal zero. Thus, an increase in limit signal will tend to reduce the required value of basic control signal and with proper choice of limit gain can prevent continued subcritical operation.

Control Parameters

Basic control pressure. - The basic control pressure selected was a diffuser static pressure p_{60} which varies essentially linearly with diffuser recovery for the conditions shown in figure 9(a). A static pressure was selected since, in general, the static pressure is more noise-free, may be measured more accurately, and tends to have better dynamic characteristics than the total pressure. The location of the pressure tap was based on several factors: the pressures upstream of the diffuser grid do not vary linearly with diffuser recovery due to choking of the grid at low recoveries; the further downstream toward the combustion zone, the shorter the dead time for response of pressure to fuel flow changes; and, finally, it was felt desirable to remain upstream of the fuel-injection zone to avoid any possible complications in pressure measurement resulting from the presence of fuel spray.

Limit pressure. - The limit signal used was the sum of two static pressures located on the diffuser innerbody on the vertical centerline in the plane of the cowl lip. The taps were positioned on the top and bottom, 180° apart, which provided a usable limit signal for both positive and negative angles of attack. Other arrangements of two or more taps could be used to include effects of both angle of attack and yaw. The variation of the limit pressure $p_{12,t+b}$ with diffuser recovery is shown in figure 9(b). The variation of $p_{12,t+b}/p_c$, as shown in figure 9(b), makes it particularly suited for a limit signal, since it is constant over almost the entire operating range and then increases sharply as maximum recovery is approached. Limiting at lower recovery could be obtained by use of pressure taps farther downstream. The figure also shows why a shock-positioning control using a single pressure-tap location cannot be used as the complete control if it is necessary to cover more than a very limited range of engine operation. For example, the shock-positioning pressure varies over its entire range at Mach 2.50 for a change in recovery of 0.004.

Reference pressure. - The reference pressure was a cone-surface static pressure located 2 inches back from the tip of the cone. The cone-surface pressure provides a limited amount of Mach number compensation. In addition, since the tap was located nominally on the horizontal centerline, the pressure should tend to drop for either positive or negative angle of attack and provide additional protection for such operation.

It should be emphasized that the various control parameters used herein are not necessarily intended to be optimum choices but are representative of pressures which could be applied in this control technique. The ultimate selection of optimum variables would necessarily be based on an extensive consideration of the performance characteristics of a specific engine and its intended application requirements, which was beyond the scope of this investigation.

Pressure - fuel flow characteristics. - The variations of the control pressures as a function of fuel flow are required to determine the engine gains necessary in the control calculations. In order to obtain these data in a more precise manner than is normally possible from curves plotted from discreet points, a continuous curve was obtained by plotting pressure as a function of fuel flow directly on an X-Y recorder, as shown in figure 10. The curves were obtained by varying the fuel flow in a linear manner from minimum to maximum and back to minimum by means of a periodic triangular input to the fuel servo with a period of 100 seconds. Note the hysteresis effect which appears, particularly in the limit traces, and also the noise level apparent even though both the pressure and fuel flow signals have been filtered with a first-order filter having a time constant of 0.1 second. Pressure - fuel flow characteristics

obtained from similar X-Y records for the flight conditions tested are shown in figure 11. The table inserted in figure 11(a) gives the pertinent information for each flight condition. The pressures shown in figure 11 are plotted for convenience as the ratio of the static pressure to the free-stream static pressure. Throughout the remainder of the report, the engine operating point is referred to in terms of this same pressure ratio.

Block Diagram and Transfer Function

Block diagram. - The complete block diagram of the control system as it was investigated is shown in figure 12. The basic loop previously discussed is shown by the heavy lines connecting blocks G_1, G_2, G_3, H_1, and H_4 and the reference R_1, obtained from p_c, A, and A_1. The remaining blocks connected by thin lines compose the limit loop. Since the limit signal consists of $p_{12,t+b}$, the two variables are taken separately and converted to equivalent voltages and then combined at the lower summing point with R_2. This value of R_2 is the limit bias previously mentioned, which is obtained as a function of p_c and is set so that the limit signal L_1 is zero for the range of diffuser recoveries shown in figure 9(b), where $p_{12,t+b}/p_c \cong 2.04$. For higher recoveries, L_2 is some negative value depending on L_1 and the gain set in block H_7 and acts to override the basic control and lower the final operating point.

Transfer function. - Each of the elements of the block diagram represents a transfer function of the output-to-input characteristics of the particular component. Each of these transfer functions may be described in terms of a frequency independent factor K and a frequency dependent factor expressed operationally, as in the case of the control $1 + 1/\tau s$ or, where based on experimental data, may be shown as a normalized frequency-response characteristic, such as that shown for $\Delta p_{60}/\Delta P_o$ in figure 4.

Each of the control-system components is shown in this manner in table I with reference to pertinent figures in the report where experimental data are available for the frequency-dependent factor. Note in table I, for the components A, H_1, H_2, and H_3, the dynamic effects of sensors and amplifiers may be neglected for the range of frequencies of concern to the control. For the components Z_1 and Z_2, which relate the limit pressures to the basic control pressure, complete dynamic information is not available. However, for the conditions under which the limit operates, that is, with the normal shock at or very near the cowl

lip, the dynamics may be approximated by a dead time of 0.01 second. This approximation appears justified on the basis of dead-time data presented in reference 7 and on careful observation of the limit pressures during sinusoidal frequency-response tests which included operation in the subcritical region, also reported in reference 7.

The open-loop transfer function of the system is derived in appendix B for conditions with the loop opened at E and with p_c, U, and $w_{f,i}$ held constant. The expression obtained is:

$$\frac{\Delta B + \Delta L}{\Delta E} = K_0\left(1 + \frac{1}{\tau s}\right)\left(\frac{\Delta p_{60}}{\Delta V_i}\right)\left[1 + \mathscr{L}K_L\left(\frac{\Delta p_{12}}{\Delta p_{60}}\right)\right]$$

where

$$K_0 = K_c K_f K_e K_s K_4$$

$$\mathscr{L} = \frac{K_7 K_l}{K_4}$$

$$K_L = K_{L,t} + K_{L,b}$$

The only factor involved in the loop gain K_0 which is not constant under normal circumstances is the engine gain K_e. The variation of this term is shown as a function of diffuser pressure ratio p_{60}/p_0 for various flight conditions in figure 13. The curves shown were obtained directly from X-Y records and represent the major variations in gain. The minor variations were removed by fairing in an average curve through the noise level of the records.

The limit gain K_L may be obtained for the various conditions directly from the slope of the curves of limit pressure ratio as a function of diffuser pressure ratios as shown in figure 14. This gain term K_L is obviously zero over most of the operating range but becomes a relatively large value in the region of limit operation.

The limit gain factor $\mathscr{L}$ has more significance than just that of a factor in the limit gain. It represents the relative magnitude of the limit signal which is combined with the basic control signal to give a resultant control signal.

PROCEDURE AND RANGE OF VARIABLES

Procedure

In order to investigate the effects of control constants on system response and stability, and to determine the effects of various engine and flight conditions on performance, the following tests were conducted. At a single engine operating point, at fixed flight conditions, and with the limit gain set at zero, the loop gain was varied from a minimum to a maximum value for various values of integrator time constants. At each setting of K_0 and τ, step disturbances in fuel servo input voltage were imposed. Response data obtained for these disturbances are also applicable to the response of the error signal to changes in the set pressure ratio. With selected values of K_0 and τ from the preceding procedure, the limit gain $\mathscr{L}$ was varied from minimum to maximum with step disturbances as before at each condition.

With selected constants of K_0, τ, and $\mathscr{L}$ from the preceding tests, the engine was operated over a range of engine and flight conditions with step disturbances in the fuel servo input voltage at each condition. The entire preceding procedure was repeated at a second Mach number.

Range of Variables

The range of flight conditions included operation at Mach 2.35 and 2.50, altitudes of 50,000, 60,000, and 65,000 feet, and angles of attack of 0 and $\pm 7^{\circ}$. The controlled engine was operated from its lean limit (fuel-air ratio of 0.037), set by the inner-ring fuel flow, to a rich limit, set by the shock-positioning limit, which allowed operation at nearly maximum diffuser recovery.

RESULTS AND DISCUSSION

The results of the control investigation are presented in a discussion of various figures showing the effects of control constants, engine operating condition, and flight condition on system performance; and a discussion of control limitations and possible improvements.

Effects of Control Constants

The transient performance of the control system is evaluated in terms of the response to a step disturbance in fuel servo input voltage. Typical system responses to a step increase and decrease in fuel servo input voltage are shown in figures 15(a) and (b), respectively. In the

oscillogram of figure 15(a), the step disturbance is imposed at point A on the fuel-servo-input-voltage trace. After a dead time of approximately 0.01 second, the fuel flow responds, followed by an additional dead time of approximately 0.02 second until the control pressure responds at point B. This total system dead time of approximately 0.03 second from A to B also appears in the V_i trace from A to C, at which point the corrective action of the control has commenced. The time required after point C to correct for the disturbance is primarily a function of the various control constants. However, regardless of the speed of the control, the system response must always include the total system dead time, in this case approximately 0.03 second.

A typical response for a step decrease in V_i resulting in overshoot is shown in figure 15(b). The quantities measured from the response are response time and percent overshoot of the fuel servo input voltage. Response time is defined herein as the time from initiation of the disturbance at point A until the control has first corrected for 90 percent of the initial error as shown by point D (fig. 15(a)). Percent overshoot is defined as (amplitude of the first overshoot/amplitude of the step) × 100, as shown in figure 15(b).

Basic-loop constants. - The effects of varying the basic-loop constants on response time and percent overshoot are shown in figure 16 for operation at Mach 2.35, altitude of 60,000 feet, and zero angle of attack. The limit gain factor $\mathscr{L}$ is set equal to zero (by setting K_7 equal to zero). The response characteristics are shown for operation with loop gains from 0.18 to 1.2 with integrator time constants ranging from 0.01 to 0.10 second. Minimum response time of 0.04 to 0.05 second with negligible overshoot may be obtained for decreasing fuel steps with a loop gain of approximately 0.6 and τ of 0.033 to 0.05 second. For increasing fuel steps, because of the nonlinearity of the pressure - fuel flow characteristics, comparable responses require a loop gain of approximately 0.7 with the same τ.

For the step decreases (fig. 16(b)) the loop gains were increased to the point where instability was reached following the disturbance, although the system was stable prior to the disturbance. In each case, the instability, as manifested by a divergent oscillation, resulted in rich blowout. A typical rich blowout resulting from unstable operation initiated by a step decrease in fuel flow is shown in figure 17.

Data for the same response at Mach 2.50 are shown in figure 18. As before, for step decreases in fuel flow, response times of 0.05 to 0.06 second with negligible overshoot may be obtained for loop gains of approximately 0.6 and τ of 0.033 to 0.05 second. For step increases, similar responses require a loop gain at approximately 0.8.

The behavior of the system at maximum loop gains for the test conditions at Mach 2.50 differed markedly from the performance at Mach 2.35. Instead of resulting in engine blowout, as shown in figure 16, operation at maximum loop gains resulted in sustained oscillations of limited amplitude, as shown in figure 19. The oscillation amplitude did not become divergent but merely increased in magnitude as the loop gain was increased. This type of instability is shown in the oscillogram of figure 20. The oscillation amplitude and frequency were measured on the control pressure trace p_{60}. The amplitude plotted in figure 19 is the peak-to-peak value shown as 198 pounds per square foot in figure 20.

The stability limits of the system were calculated from the experimental open-loop frequency-response characteristics on the basis of linear stability theory. Experimental frequency-response data for the response of the control signal $V_{p_{60}}$ to the fuel servo input voltage V_i are shown in figure 21 for test conditions closely matching those for which stability data have been presented at Mach 2.35 and 2.50. The control characteristic $1 + 1/\tau s$ is shown separately in order to allow determination of the stability limits for each of the integrator rates tested. The intersection of the curve for $-(180^\circ + \theta)$ in figure 21(b) with those of various τ indicates the frequency of instability for the particular set of conditions. The gain at which the system will become unstable is determined from figure 21(a) and is the factor which is required to make the product of $(\Delta V_{p_{60}}/\Delta V_i)$ times the control amplitude equal to one at the frequency indicated from the phase characteristics. For example, at Mach 2.35 for $\tau = 0.05$, the frequency of instability is approximately 16.4 cps (fig. 21(b)); the amplitudes of $\Delta V_{p_{60}}/\Delta V_i$ and $1 + 1/\tau s$ at 16.4 cps (from fig. 21(a)) are 0.69 and 1.05, respectively; the stability limit-loop gain is, therefore, $1/(1.05 \times 0.69) = 1.385$.

The calculated limits are summarized and compared with the experimental limits in figure 22. There is reasonable agreement in frequency for all the data and also in the data for loop gain at Mach 2.50. However, the experimental data for loop gain at Mach 2.35 are consistently lower than calculated. The gain is lower at this Mach number because it was not the gain required to give instability in steady state, but resulted in instability only after a step decrease which effectively increased the engine gain and also the loop gain. In contrast, the maximum loop gains at Mach 2.50 were obtained by increasing the loop gain during steady-state operation until instability was reached without any disturbance except the normal system noise.

Limit-loop constants. - The effect of the limit loop on the transient response is shown in the three oscillograms of figures 23(a), (b), and (c) for limit gains $\mathscr{L}$ of 0, 0.357, and 0.663, respectively. As $\mathscr{L}$ is increased, the response time is decreased (figs. 23(a) and (b)) and eventually results in a large amount of overshoot (fig. 23(c)). However, for

the particular operating conditions shown, the limit operation does not change the length of time the engine remains subcritical, as shown by the duration of the pulse in the limit-signal trace. This condition is a result of operation at low supercritical diffuser pressure recovery and the fact that the basic control response is fairly fast. As a result, before the limit signal may become effective (due to the system dead time), the corrective action of the basic control has returned the engine to the supercritical region. For operation at higher recovery, where the engine is operating subcritically during most of the transient, the limit action significantly reduces the subcritical operating time, as shown in figure 24. The period of subcritical operation, corresponding to the duration of limit-signal pulse shown in figure 24, is reduced from 0.22 second with limit gain equal to zero to a minimum of approximately 0.062 second with larger values of limit gain.

The effects on system response of varying the limit gain for operation at Mach 2.35 and 2.50 are shown in figures 25(a) and (b), respectively. When the initial operating point was set just below the level of limit operation (fig. 25(a)), increasing the limit gain resulted in sustained oscillations at 10.2 cps at a gain of 0.625. For a further supercritical operating point (fig. 25(b)), the limit gain was safely raised to over 1.0. In both sets of data, the trends are the same as the gain is increased, that is, a rapid reduction in response time for step increases in fuel flow until a minimum value is reached of approximately 0.04 to 0.055 second, followed by an increase in the overshoot.

The difference in optimum $\mathscr{L}$ settings (0.125 in fig. 25(a) and 0.35 in fig. 25(b)) is mainly due to the different operating levels. That is, for conditions shown in figure 25(a), the control was set at a high diffuser pressure level, where limit operation was effective during most of the transient; and, at conditions shown in figure 25(b), the control was set for a much lower relative value, where the limit operated for a comparatively short time during the transient. The lower value of $\mathscr{L}$ is more significant since the limit operation will be most critical for operation at near maximum diffuser pressure ratios, in particular at pressure ratios that result in the average value of the limit signal being greater than zero (referred to as continuous limit operation). As will be shown subsequently, for those conditions requiring continuous limit operation, the restrictions on maximum gain are even more severe.

Effects of Disturbance Size and Operating Point

Disturbance size. - The effect of increasing the size of the fuel flow disturbance is shown in figure 26 for operation with constant control settings. The general effect of increasing the disturbance size was to gradually increase the response time and reduce the percent

overshoot. This is due to the nonlinearity of the engine characteristics, which results in nearly a constant maximum available error signal regardless of disturbance size for all disturbances resulting in operation at, or beyond, peak recovery. In spite of the previously mentioned effects, the control was able to recover from disturbances which placed the engine temporarily well beyond the steady-state blowout limits. For example, at Mach 2.35 (fig. 26(a)), the steady-state engine blowout limits correspond to an increase of approximately 0.52 pound per second and yet, as shown, it required an increase of 0.73 pound per second or larger to blow out on control. At Mach 2.50 (fig. 26(b)), the steady-state limits correspond to an increase of 1.09 pounds per second, and the control recovered from disturbances up to 2.62 pounds per second.

Operating point. - The performance of the system with constant control settings over the range of diffuser pressure ratios at constant Mach number varied considerably because of variations in the engine gain and the effects of limit operation. As shown in figure 27, the control constants selected provided minimum response time with small overshoot at pressure ratios slightly below the level of continuous limit operation. With these same control settings the response time remained essentially constant at nearly the minimum value over the range of pressure ratios shown. The percent overshoot, however, tended to increase because of the increase in engine gain at the lower pressure ratios and the limit action at higher ratios.

Although the control operated over the range of conditions shown in figure 27 and provided fast response at all conditions, the operation was accompanied by a considerable degree of instability, as indicated by the wide variation in percent overshoot. Actually, much of the operation was accomplished in the presence of sustained oscillations of limited amplitude resulting from the increases in engine gain, the effects of limit operation, and also from the normal variation of engine and fuel-system noise level, which, at particular conditions, appeared to be strongly resonant at discreet frequencies.

These variations in oscillation amplitude and frequency are shown in figure 28. (The engine noise level with the control off is shown at several conditions by the square symbols.) The predominant frequency observed at each condition does not necessarily correspond to that which may be expected from the stability data previously shown. Instead, there appear to be at least three principal bands of frequency, any one of which may be the dominant one; or, as shown in figure 28(a), at p_{60}/p_0 of 8.26 two bands may be observed at the same condition. An example of this situation may be seen in the oscillogram shown in figure 29. In this oscillogram the system has an initial frequency of oscillation of approximately 12.2 cps, and following a step disturbance has a frequency of oscillation of approximately 34.7 cps.

The effect of continuous limit operation on the system stability is readily apparent from the frequency-response curves (fig. 30). The response characteristics of the system without the limit indicate the system would be stable. That is, the amplitude is less than 1.0 at a phase shift of 180° (14.7 cps). However, with the limit included, the amplitude is 2.0 at the 180° phase-shift point (10.7 cps). In addition, the amplitude is still greater than 1.0 at the 540° phase-shift point (32.5 cps), which corresponds to the second frequency observed. The third frequency band observed in the tests (100 to 105 cps) corresponds to a resonant peak observed in the engine response but for which no precise data could be obtained as to amplitude or phase shift.

Effects of Flight Conditions

Operation of the control system over the range of flight conditions tested was accompanied by considerable variations in performance (resulting from variations in engine characteristics) as described in the following sections.

Altitude and Mach number. - The dynamic performance of the system at various altitudes and Mach numbers was primarily a function of the engine and limit-gain characteristics, which are shown in figures 13 and 14 and varied with both altitude and Mach number. Variations in engine dynamics were observed at different flight conditions; however, no definite trend could be established for these changes. In any case, the changes observed were, in general, sufficiently minor so that the engine and limit gains remained the principal variables to be considered in determining response and stability characteristics.

Angle of attack. - Operation of the engine at various angles of attack presented several problems such as variation in reference pressure, changes in static characteristics of control and limit pressures, and conflicting requirements on the gain of the limit loop. These factors are discussed in detail in the following section.

In spite of the problems mentioned, successful operation of the control (with respect to preventing blowout at angle of attack) was achieved for all conditions tested. An example of control operation during a transient for $\alpha = 0$ to $+7^\circ$ is shown in figure 31. At the initial conditions at $\alpha = 0$, the control was holding p_{60}/p_0 at 9.68, the reference pressure was $p_c/p_0 = 2.82$, and the limit signal was zero. As the transient progressed, the reference pressure decreased and the limit became effective. At $\alpha = +7^\circ$, the reduced reference pressure would have resulted in setting $p_{60}/p_0 = 9.2$, which exceeds the steady-state limits at $\alpha = +7^\circ$ of $p_{60}/p_0 = 9.1$. Thus, the effectiveness of the limit is observed in the reduction of p_{60}/p_0 held to 8.86, safely below the allowable limits.

Control Limitations and Possible Improvements

Reference pressure. - Although the reference pressure provided partial compensation for Mach number, it was not entirely satisfactory for operation at angle of attack. Due to the fact that the reference tap was located slightly off the horizontal centerline, operation at positive angles of attack resulted in a desirable reduction of the reference pressure; but negative angles of attack resulted in an increase, which required greater limit action than would have normally been necessary.

It is possible that a combination of static or total cone pressures such as used in reference 4 could be selected to provide the desired variation of reference pressure with Mach number and angle of attack.

Basic control pressure. - The particular control pressure used appears to be as suitable as any diffuser pressure available in the engine tested. A comparison of the dynamic characteristics of several diffuser static pressures, as reported in reference 7, reveals no major differences, although, in general, the farther downstream in the diffuser the tap is located, the shorter the dead time. For this engine, at least, the variation is not sufficient to cause any marked change in control performance. For example, the pressure at station 36 was also tested in the control and the resulting control responses, when plotted as a function of loop gain and integrator time constant, fall within the experimental scatter of data for the control responses obtained with the static pressure at station 60.

The main difference between the various stations appeared to be in the relative linearity and consequent variations encountered in engine gain. In this respect the X-Y recorder technique employed to obtain steady-state pressure - fuel flow characteristics proved a desirable method for evaluating the potentialities of various pressures as control parameters. For example, the static pressure at station 36, which was tested in the control and found to have minor dynamic differences with respect to the pressure at station 60, when plotted on the X-Y recorder was found to have numerous nonlinearities which made it almost impossible to obtain precise values of engine gain.

Limit pressure. - The difficulties encountered with the limit signal used are principally related to operation at angle of attack. Characteristics of the diffuser at Mach 2.50 and an altitude of 60,000 feet are shown in figure 32 for 0 and $\pm 7^{\circ}$ angles of attack. The difference in the curves for $\pm 7^{\circ}$ are attributed to the nonsymmetry of the diffuser resulting from a main engine support strut. The maximum available limit signal at angle of attack (fig. 32(a)) makes it necessary to set the limit gain factor $\mathscr{L}$ large enough to make $\mathscr{L}(\Delta p_{12,t+b}) = \Delta p_{60}$, assuming a constant reference pressure.

For example, in figure 32 if p_{60}/p_0 set at $\alpha = 0$ is 9.6, then $p_{12,t+b}/p_0$ is 5.7. At $\alpha = +7^\circ$, maximum p_{60}/p_0 is 9.1 and maximum $p_{12,t+b}/p_0$ is 7.6. Then, $\Delta(p_{60}/p_0)$ is 9.6 - 9.1 or 0.5 and maximum $\Delta(p_{12,t+b}/p_0)$ is 7.6 - 5.7 or 1.9. Therefore, $\mathscr{L}$ must be at least 0.5/1.9 or 0.263 to provide sufficient limit signal to prevent blowout. However, for the data shown in figure 29, the system would be unstable for operation at $\alpha = 0$ with continuous limit action for $\mathscr{L}$ greater than approximately 0.09. That is, maximum $\mathscr{L}$ approximately equals 0.1785/2 = 0.089, where 0.1785 is $\mathscr{L}$ from figure 30 and 2 is the amplitude at the frequency of instability (10.8 cps). This value of maximum $\mathscr{L}$ is only approximate, but it is indicative of the discrepancy between a suitable limit gain for stable operation with continuous limit action and a sufficient limit gain to permit operation at angle of attack.

A possible solution to the problem would be to allow the control to be unstable for continuous limit operation and provide the necessary gain for protection during angle-of-attack operation. This might be feasible under some circumstances, since even with the system in a sustained oscillation the control was capable of recovering from other disturbances, as shown in figure 27.

Another possibility would be to provide for stable limit operation at high recovery and to provide angle-of-attack protection by appropriate choice of a reference pressure which varies with angle of attack in the required manner.

A third possible solution is to slow down the limit loop so as to stabilize it for normal operation at high recovery but still permit the use of a loop gain high enough for effective action at angle of attack. For this engine, at least, this might be the most desirable solution, since during a transient the limit cannot prevent momentary subcritical operation nor even reduce the maximum deviation encountered during the first part of the transient. This situation arises because the dynamics of the engine other than dead time are minor as compared with the total system dead time. This means essentially that for any step disturbance the engine has time to shift to a new operating point corresponding to the disturbance before any corrective action from the control has an opportunity to become effective.

The slowing down of the limit loop without impairing the response of the control system may be accomplished as shown in figure 33. The upper curve in figure 33(a) shows the characteristics of the complete system with a value of $\mathscr{L}$ of 0.268, which is adequate to provide the necessary limit action at $\alpha = +7^\circ$, as previously shown. The lower curve is the same system with the addition of a first-order lag in the

limit loop with τ_{lg} of 0.062 second. This gives the limiting case in which at 180° phase shift (7 cps) the amplitude has been reduced to just under 1.0. Thus, for the conditions shown, τ_{lg} of 0.062 second or larger would stabilize the limit loop at zero angle of attack and allow the use of sufficient gain for angle-of-attack protection.

The addition of the lag would lower the effectiveness of the limit to reduce the period of subcritical operation for disturbances at high recovery, as shown in figure 24. However, the higher allowable limit gains would tend to compensate for this reduced effectiveness, and it is possible that the net effect would not seriously impair the response characteristics at high recovery.

CONCLUDING REMARKS

Results have been presented from an investigation of a diffuser static-pressure-ratio control with a normal shock-positioning limit for a range of engine, flight, and control conditions. Based on the results presented, the following remarks may be made.

The dynamics of the engine were such that the control was unable to limit the magnitude of the initial deviation of the control pressure resulting from a step disturbance in fuel flow. However, it is significant to note that short periods of operation during a transient beyond the steady-state blowout limits does not necessarily result in immediate engine blowout. It appears that a finite period of time is required to result in blowout, as evidenced by the fact that successful recovery was made, with the control system tested, from disturbances which placed the engine well beyond the steady-state blowout limits.

The operation of the basic control was affected primarily by the variations of engine gain encountered over the range of test conditions which precluded optimum response characteristics at all conditions with fixed control settings. With optimum control constants, response times of 0.04 to 0.06 second were obtained with small amounts of overshoot at a single condition. Comparable response times were obtained over a broad range of test conditions; however, the overshoot varied widely for the range of test conditions.

It appears that, if the degree of instability encountered can be tolerated, the basic control may be operated successfully over a broad range of conditions with fixed constants to provide minimum response times or, conversely, more stable operation over the same range of conditions may be obtained by allowing somewhat slower response times. The alternative is to vary the control constants as a function of engine and flight conditions, which adds obvious complexity to the system.

The shock-positioning limit was effective in reducing the control response time for disturbances which placed the engine in the subcritical region. For operation at high recovery, the limit effectively reduced the duration of subcritical operation for such disturbances. At lower recovery, although still contributing effectively to lower response time, the limit had negligible effect on the duration of subcritical operation.

In order to ensure safe limiting action at angle of attack, it was necessary to set the limit gain at a relatively high value, which resulted in sustained oscillations during continuous limit operation. However, it appeared possible to stabilize the limit loop, without seriously impairing its normal operation, by the addition of a suitable first-order lag, which will allow stable continuous limit operation with gains sufficiently large to ensure safe limit action at angle of attack.

Lewis Flight Propulsion Laboratory
National Advisory Committee for Aeronautics
Cleveland, Ohio, July 25, 1956

APPENDIX A

SYMBOLS

A	reference input element in control system
B	basic control-loop feedback signal
E	control actuating error signal
G	control-system element in forward direction
H	feedback element in control system
h	altitude, ft
K	gain factor, independent of frequency
K_o	loop gain as derived in appendix B
L	limit-loop feedback signal
$\mathscr{L}$	limit-loop gain factor
M	Mach number
P	total pressure, lb/sq ft abs
P_o	pressure drop across outer-ring fuel nozzle, lb/sq in.
p	static pressure, lb/sq ft abs
R	reference input to control
s	Laplace operator
T	inlet-air total temperature, ^oF
U	step-function input to control
V	voltage, v
V_f	fuel-valve-position voltage, v
V_i	fuel servo input voltage, v
V_o	control output voltage, v

w_a	air flow, lb/sec
w_f	total fuel flow, lb/sec
$w_{f,i}$	fuel flow, inner-ring manifold, lb/sec
$w_{f,o}$	fuel flow, outer-ring manifold, lb/sec
Z	indirectly controlled system element
α	angle of attack, deg
θ	angle of phase shift, deg
τ	integrator time constant, sec
τ_{lg}	time constant of lag, sec

Subscripts:

b	bottom
c	cone surface, 2 in. downstream of cowl lip
t	top
0	free stream
1	engine inlet
2	diffuser exit
0,2,12, 36,60,80	engine stations, inches downstream of tip of cone

APPENDIX B

CONTROL-SYSTEM TRANSFER FUNCTION

The open-loop transfer function for the control system opened at E (fig. 12) and with p_c, U, and $w_{f,i}$ constant may be written as follows:

$$\Delta B = (\Delta E)G_1G_2G_3H_1H_4 \tag{1}$$

and

$$\Delta L = (\Delta E)G_1G_2G_3H_7(Z_1H_3H_6 + Z_2H_2H_5) \tag{2}$$

Adding equations (1) and (2) and factoring yield

$$\Delta B + \Delta L = (\Delta E)G_1G_2G_3\left[H_1H_4 + H_7(Z_1H_3H_6 + Z_2H_2H_5)\right] \tag{3}$$

or, rewriting,

$$\frac{\Delta B + \Delta L}{\Delta E} = G_1G_2G_3H_1H_4\left[1 + \frac{H_7}{H_1H_4}(Z_1H_3H_6 + Z_2H_2H_5)\right] \tag{4}$$

From table I it may be seen that

$$H_1 = H_2 = H_3 = K_s$$

$$H_5 = H_6 = K_l$$

$$\frac{\Delta p_{12,b}}{\Delta p_{60}} = \frac{\Delta p_{12,t}}{\Delta p_{60}} = \frac{\Delta p_{12}}{\Delta p_{60}}$$

From these relations and by substituting the appropriate terms from table I in equation (4),

$$\frac{\Delta B + \Delta L}{\Delta E} = K_c\left(1 + \frac{1}{\tau s}\right)K_f\left(\frac{\Delta w_{f,o}}{\Delta V_i}\right)K_e\left(\frac{\Delta p_{60}}{\Delta w_{f,o}}\right)K_sK_4 \times$$

$$\left[1 + \frac{K_7K_5}{K_4}(K_{L,t} + K_{L,b})\left(\frac{\Delta p_{12}}{\Delta p_{60}}\right)\right] \tag{5}$$

5043

or, by rewriting,

$$\frac{\Delta B + \Delta L}{\Delta E} = K_c K_f K_e K_s K_4 \left(1 + \frac{1}{\tau s}\right)\left(\frac{\Delta p_{60}}{\Delta V_i}\right) \times \left[1 + \frac{K_7 K_l}{K_4}\left(K_{L,t} + K_{L,b}\right)\left(\frac{\Delta p_{12}}{\Delta p_{60}}\right)\right] \tag{6}$$

Let

$$\frac{K_7 K_l}{K_4} = \mathscr{L}$$

$$K_{L,t} + K_{L,b} = K_L$$

$$K_c K_f K_e K_s K_4 = K_0$$

Then,

$$\frac{\Delta B + \Delta L}{\Delta E} = K_0 \left(1 + \frac{1}{\tau s}\right)\left(\frac{\Delta p_{60}}{\Delta V_i}\right)\left[1 + \mathscr{L} K_L \left(\frac{\Delta p_{12}}{\Delta p_{60}}\right)\right] \tag{7}$$

REFERENCES

1. Boksenbom, Aaron S., and Novik, David: Control Requirements and Control Parameters for a Ram Jet with Variable-Area Exhaust Nozzle. NACA RM E8H24, 1948.

2. Himmel, Seymour C.: Some Control Considerations for Ram-Jet Engines. NACA RM E52F10, 1952.

3. Vasu, G., Wilcox, F. A., and Himmel, S. C.: Preliminary Report of Experimental Investigation of Ram-Jet Controls and Engine Dynamics. NACA RM E54H10, 1954.

4. Dunbar, William R., Vasu, George, and Hurrell, Herbert G.: Experimental Investigation of Direct Control of Diffuser Pressure on 16-Inch Ram-Jet Engine. NACA RM E55D15, 1955.

5. Hurrell, Herbert G., Vasu, George, and Dunbar, William R.: Experimental Study of Shock-Positioning Method of Ram-Jet-Engine Control. NACA RM E55F21, 1955.

6. Vasu, George, Hart, Clint E., and Dunbar, William R.: Preliminary Report on Experimental Investigation of Engine Dynamics and Controls for a 48-Inch Ram-Jet Engine. NACA RM E55J12, 1956.

7. Wentworth, Carl B., Dunbar, William R., and Crowl, Robert J.: Altitude Free-Jet Investigation of Dynamics of a 28-Inch-Diameter Ram-Jet Engine. NACA RM E56F28b, 1956.

8. Otto, Edward W., Gold, Harold, and Hiller, Kirby W.: Design and Performance of Throttle-Type Fuel Controls for Engine Dynamics Studies. NACA TN 3445, 1955.

CONFIDENTIAL

TABLE I. - SUMMARY OF CONTROL-SYSTEM COMPONENTS

Element (fig. 12)	Transfer function	Remarks
A	$K_s\left(\frac{\Delta V_{p_c}}{\Delta p_c}\right)$	$\left(\frac{\Delta V_{p_c}}{\Delta p_c}\right) = 1$ for frequencies of interest in control study (fig. 7)
A_1	$K_{A,1}$	
A_2	$K_{A,2}$	
G_1	$K_c(1 + 1/\tau s)$	K_c and τ variable as desired (fig. 21)
G_2	$K_f(\Delta w_{f,o}/\Delta V_i)$	$K_f = 0.520$ (lb/sec)/v, $\Delta w_{f,o}/\Delta V_i$ (fig. 5)
G_3	$K_e(\Delta p_{60}/\Delta w_{f,o})$	K_e variable (fig. 13), $\Delta p_{60}/\Delta w_{f,o}$ (fig. 4)
H_1	$K_s(\Delta V_{p_{60}}/\Delta p_{60})$	$(\Delta V_{p_{60}}/\Delta p_{60}) = 1$ for frequencies of interest (fig. 7)
H_2	$K_s(\Delta V_{p_{12,b}}/\Delta p_{12,b})$	$(\Delta V_{p_{12,b}}/\Delta p_{12,b}) = 1$ for frequencies of interest (fig. 7)
H_3	$K_s(\Delta V_{p_{12,t}}/\Delta p_{12,t})$	$(\Delta V_{p_{12,t}}/\Delta p_{12,t}) = 1$ for frequencies of interest (fig. 7)
H_4	K_4	
H_5	K_5	$K_5 = K_1$
H_6	K_6	$K_6 = K_1$
H_7	K_7	
Z_1	$K_{L,t}(\Delta p_{12,t}/\Delta p_{60})$	$(\Delta p_{12,t}/\Delta p_{60}) = e^{-0.01s}$
Z_2	$K_{L,b}(\Delta p_{12,b}/\Delta p_{60})$	$(\Delta p_{12,b}/\Delta p_{60}) = e^{-0.01s}$

Note: All terms in parenthesis are dimensionless functions of frequency.

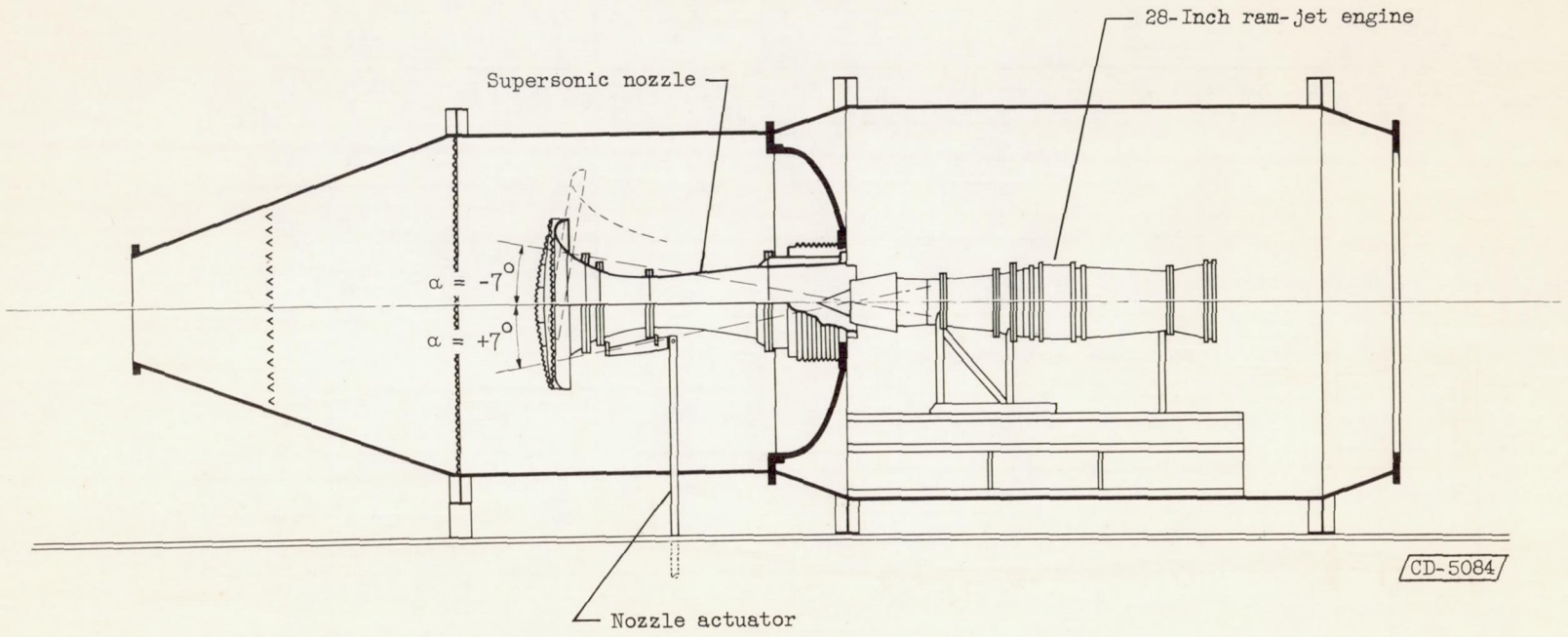

Figure 1. - Installation of 28-inch ram-jet engine in altitude free-jet facility.

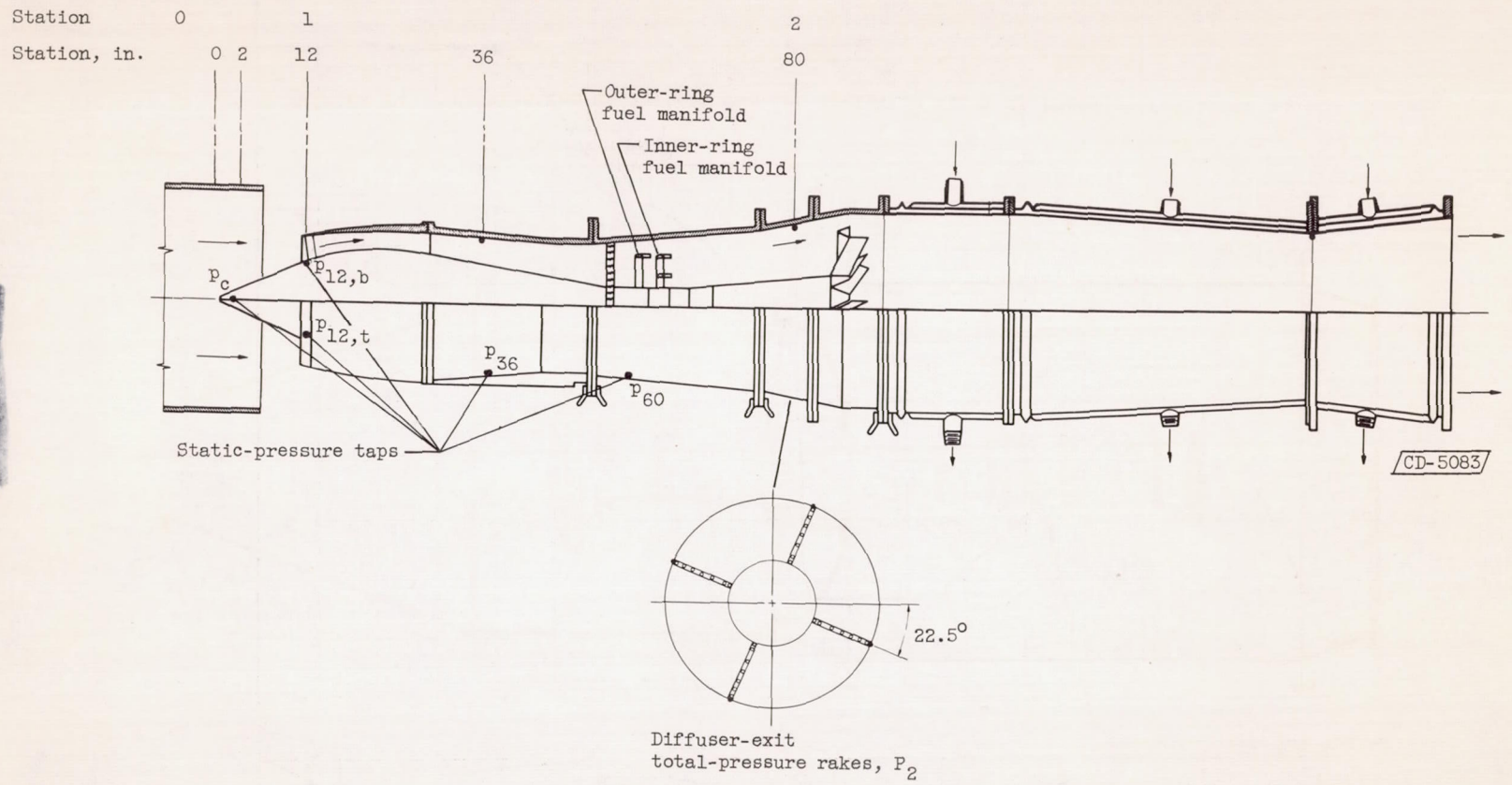

Figure 2. - 28-Inch ram-jet engine and location of instrumentation.

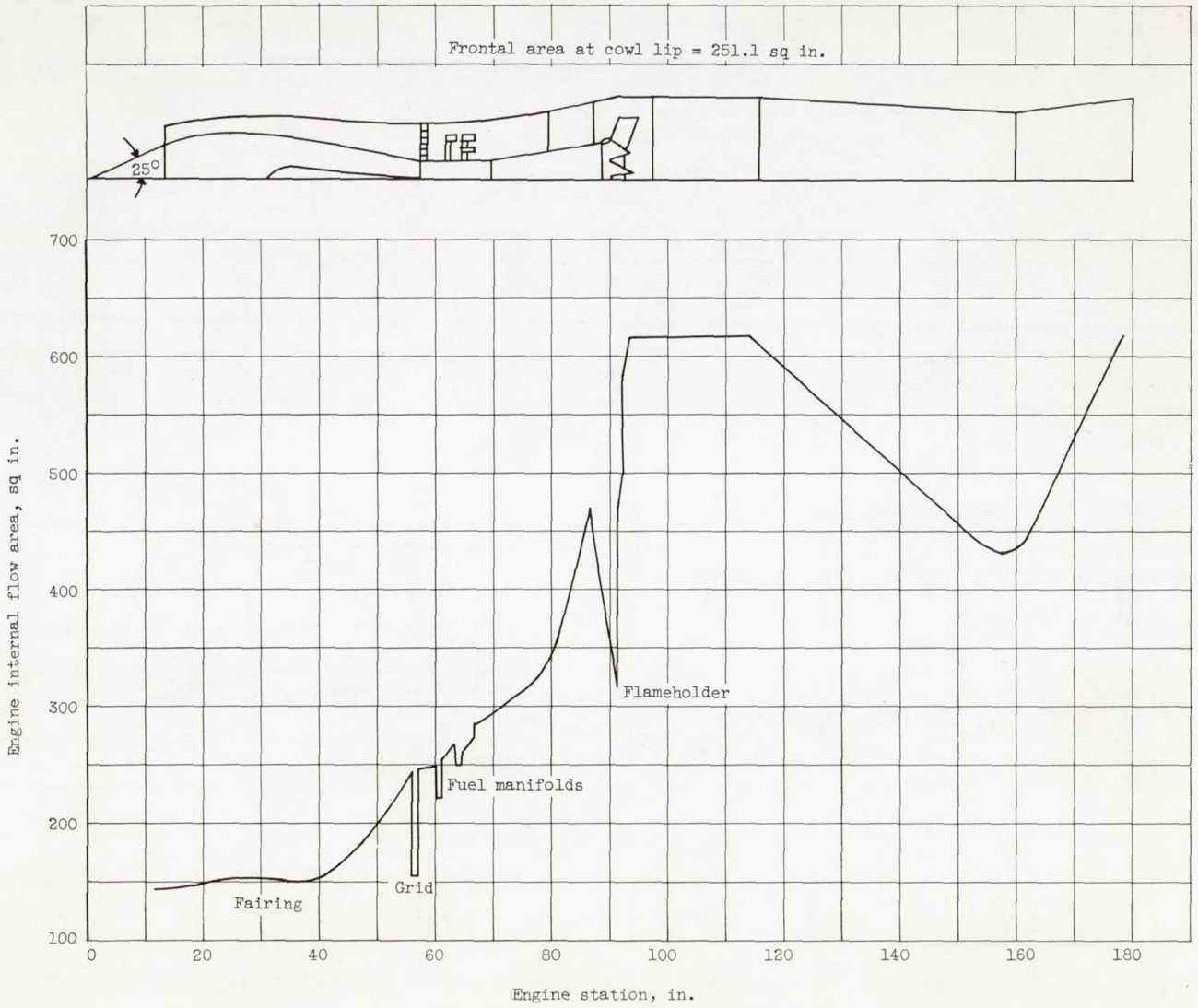

Figure 3. - Area variation of 28-inch ram-jet engine.

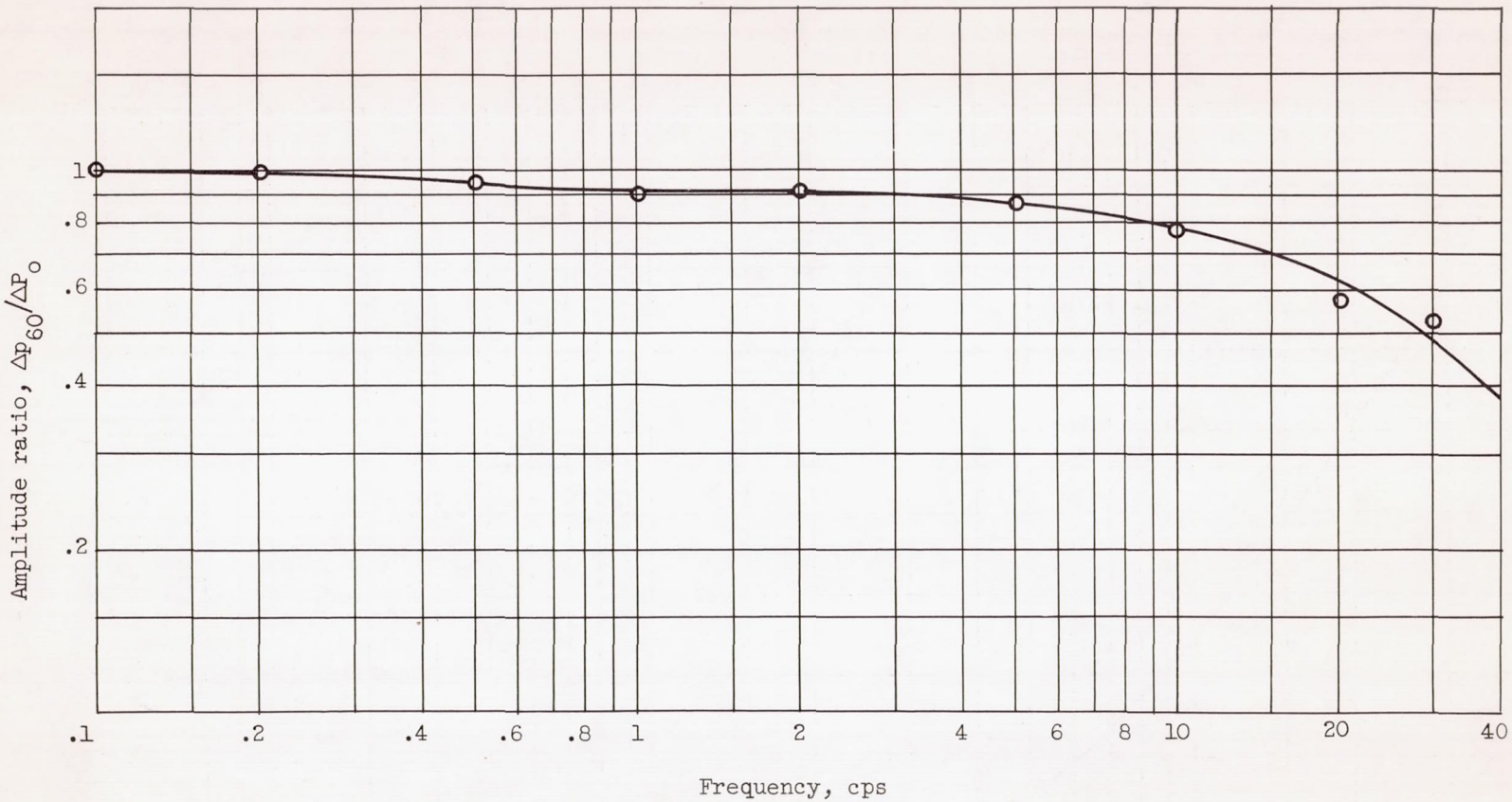

(a) Amplitude ratio.

Figure 4. - Typical frequency-response characteristics of diffuser static pressures to fuel flow.

(b) Phase shift.

Figure 4. - Concluded. Typical frequency-response characteristics of diffuser static pressures to fuel flow.

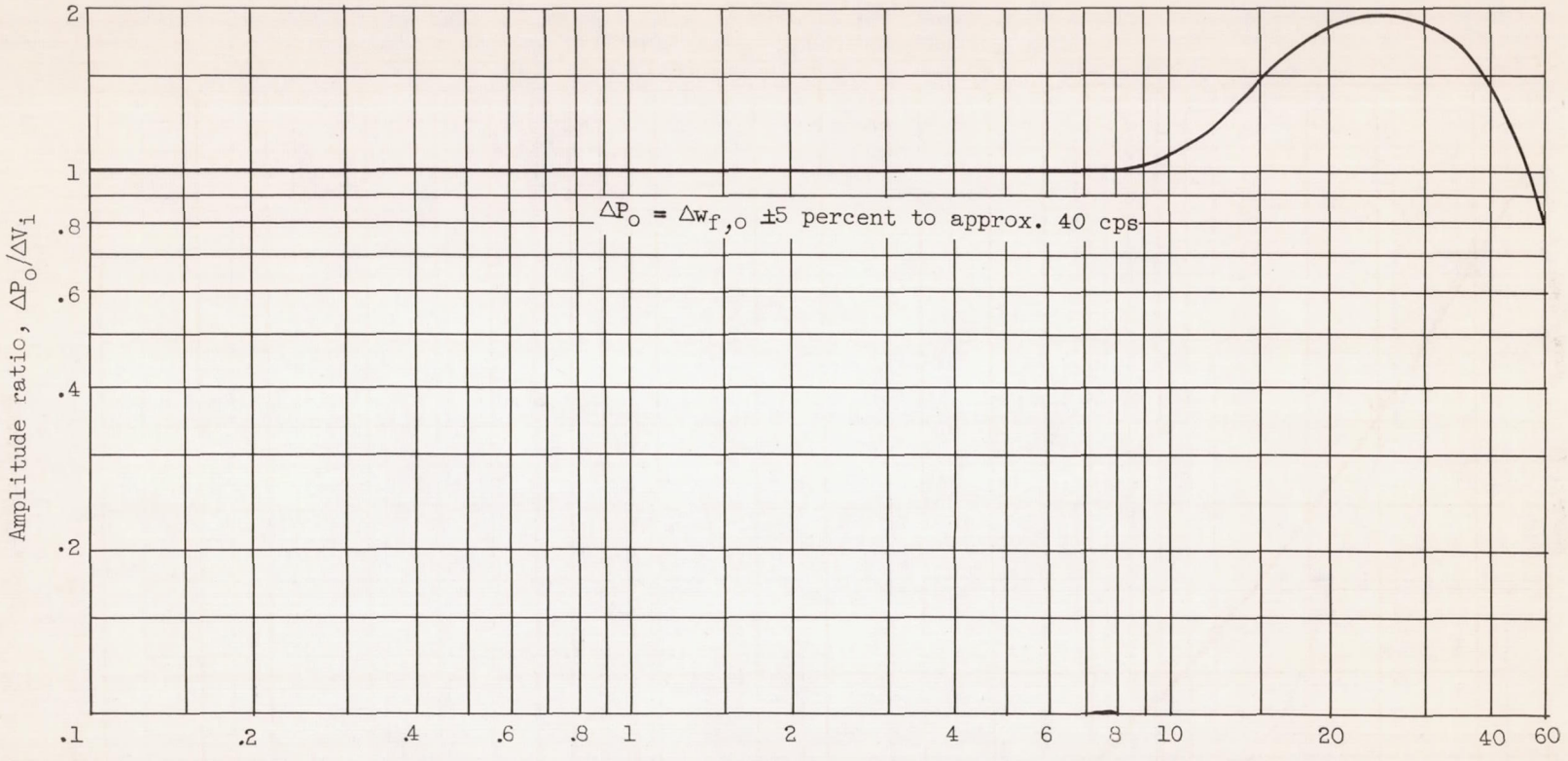

(a) Amplitude ratio.

Figure 5. - Typical frequency-response characteristics of fuel system.

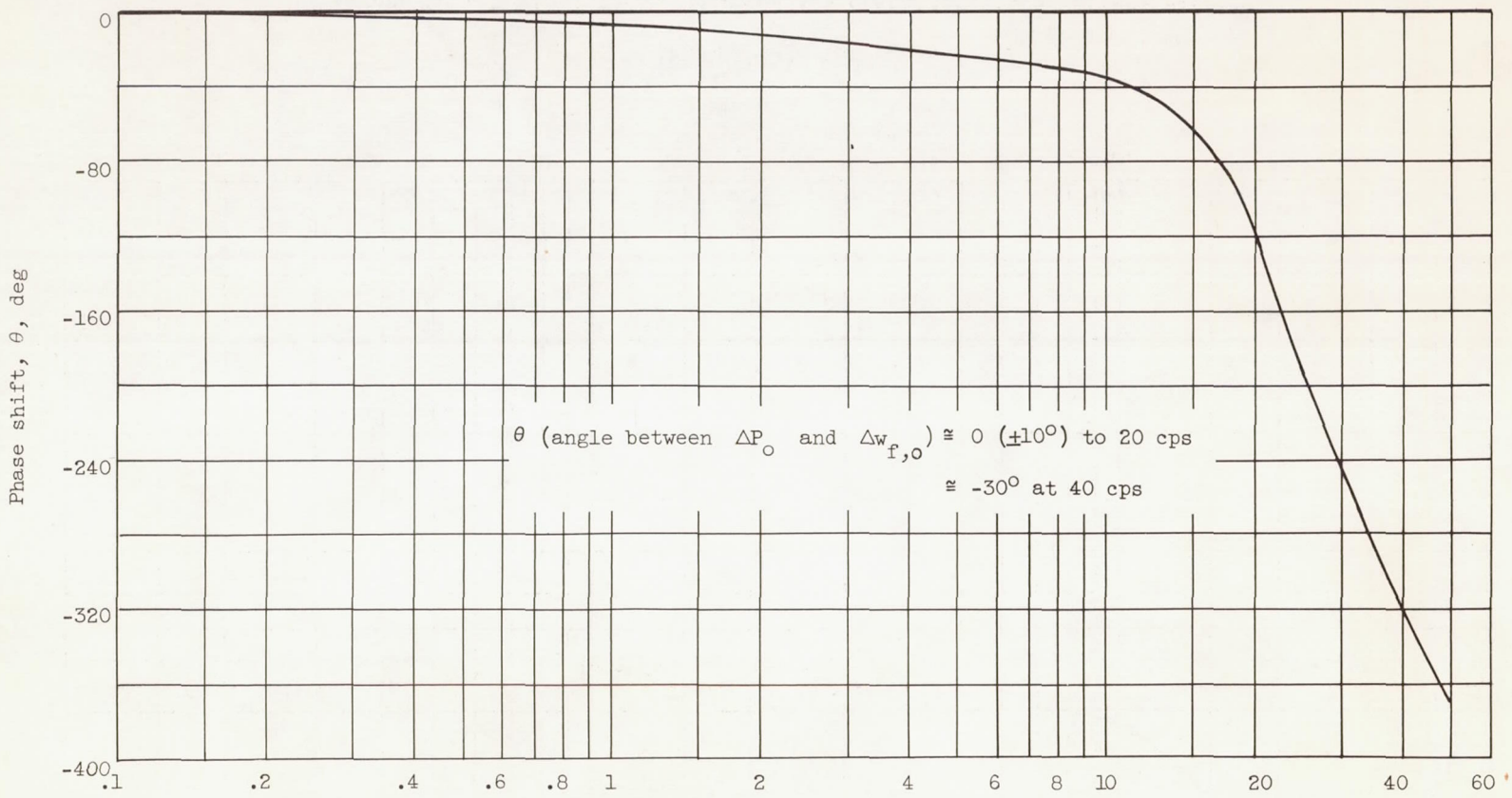

(b) Phase shift.

Figure 5. - Concluded. Typical frequency-response characteristics of fuel system.

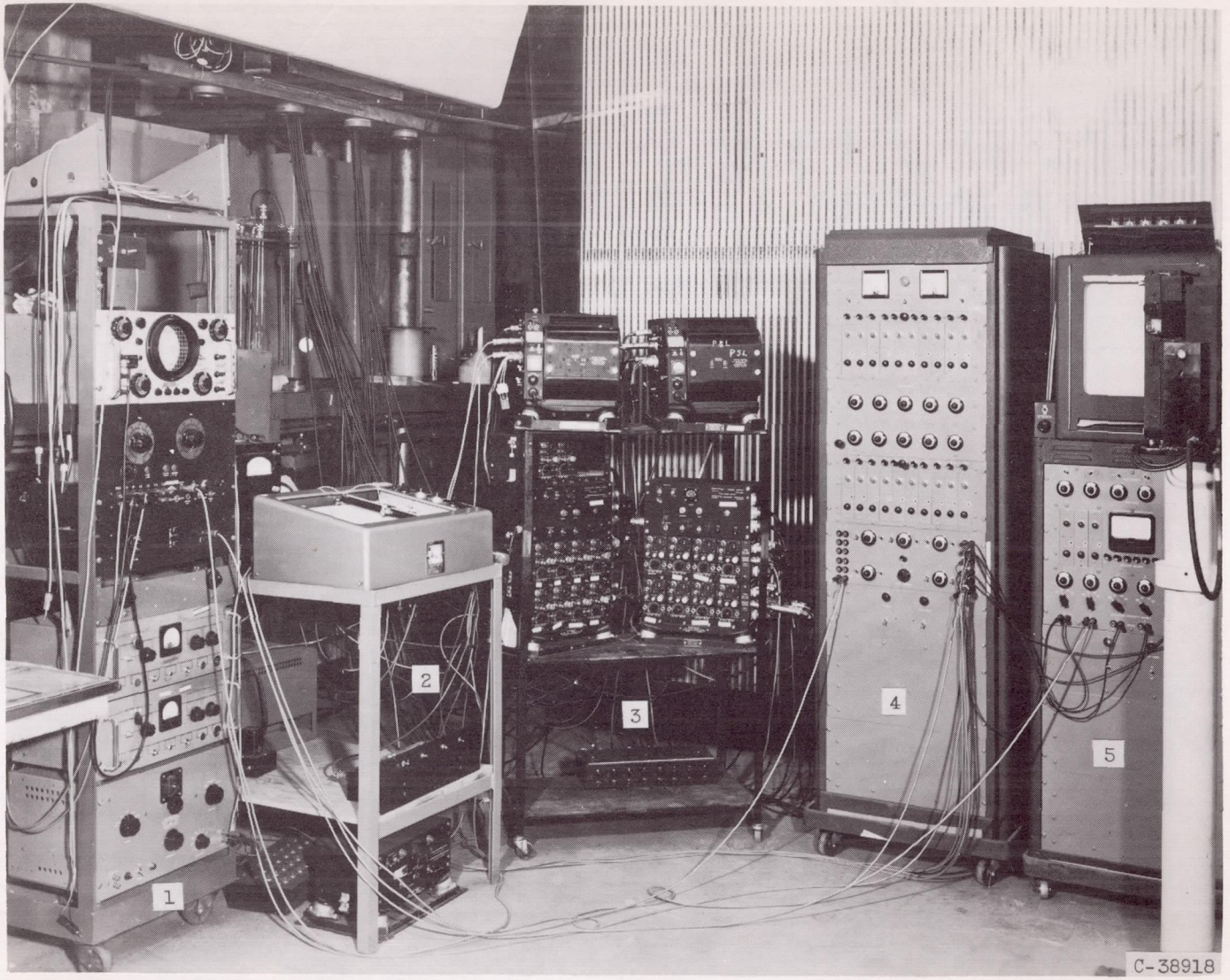

Figure 6. - Control computer and recording equipment.

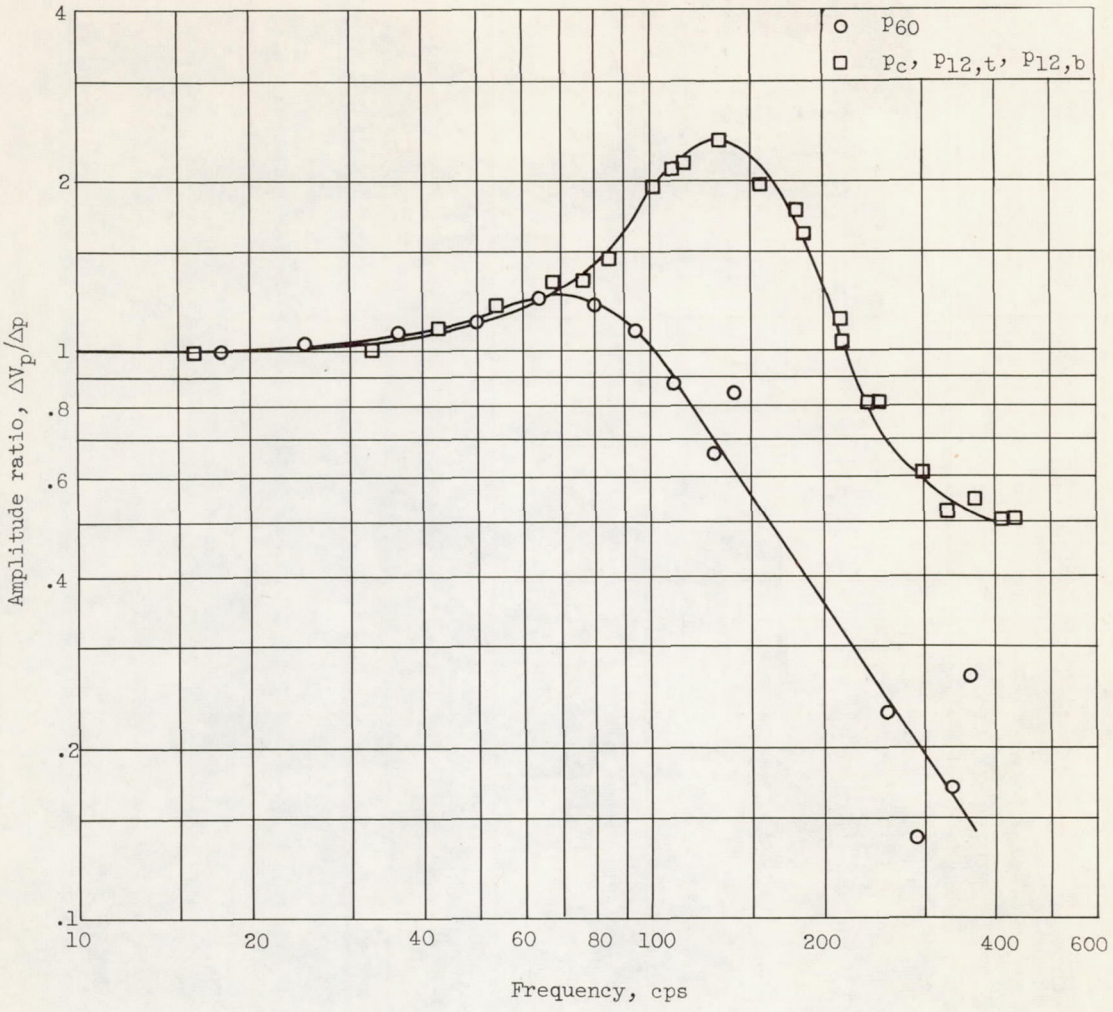

(a) Amplitude ratio.

Figure 7. - Frequency-response characteristics of engine pressure transducers. Pickup, 9 inches of 0.040-inch-inside-diameter tubing.

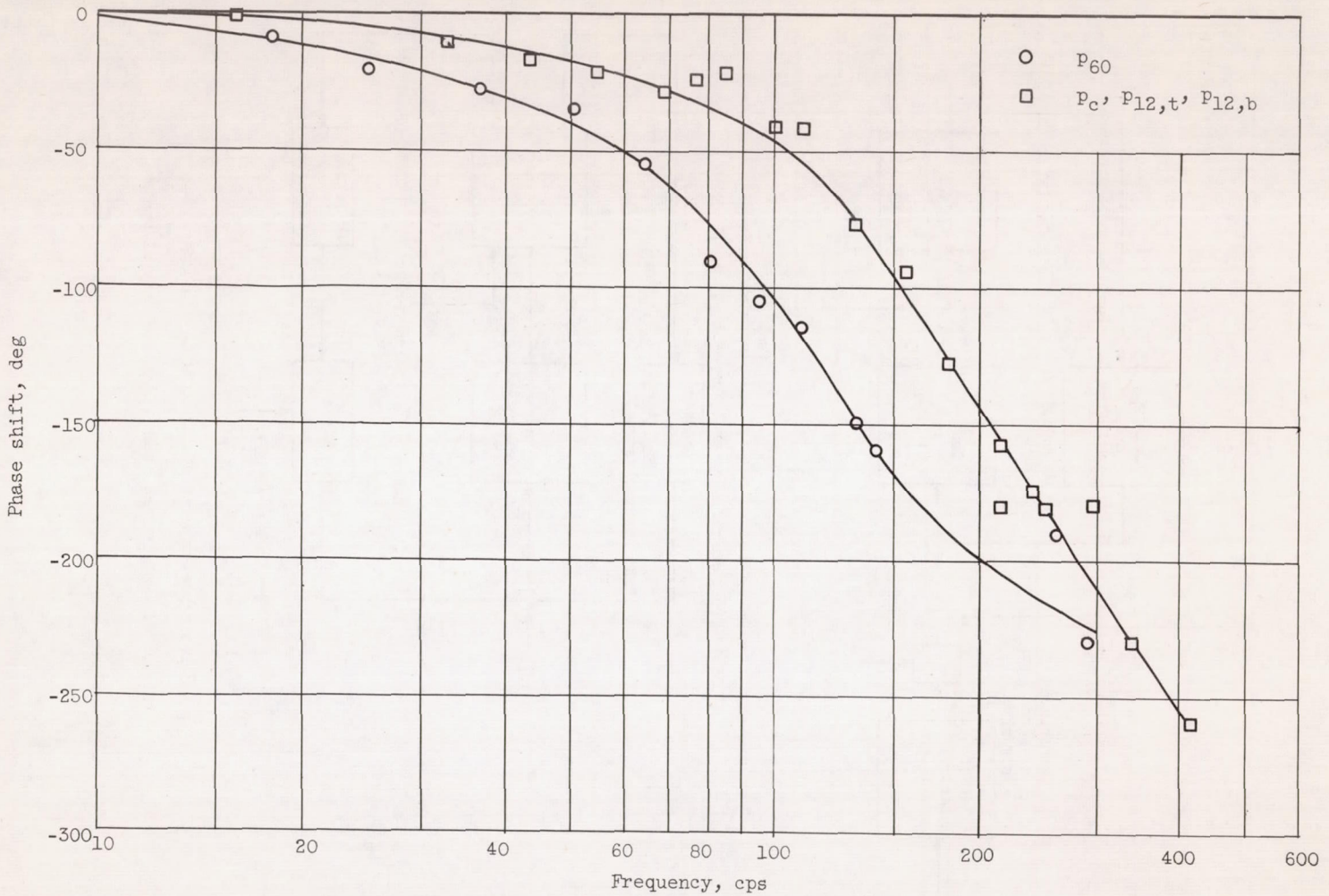

(b) Phase shift.

Figure 7. - Concluded. Frequency-response characteristics of engine pressure transducers. Pickup, 9 inches of 0.040-inch-inside-diameter tubing.

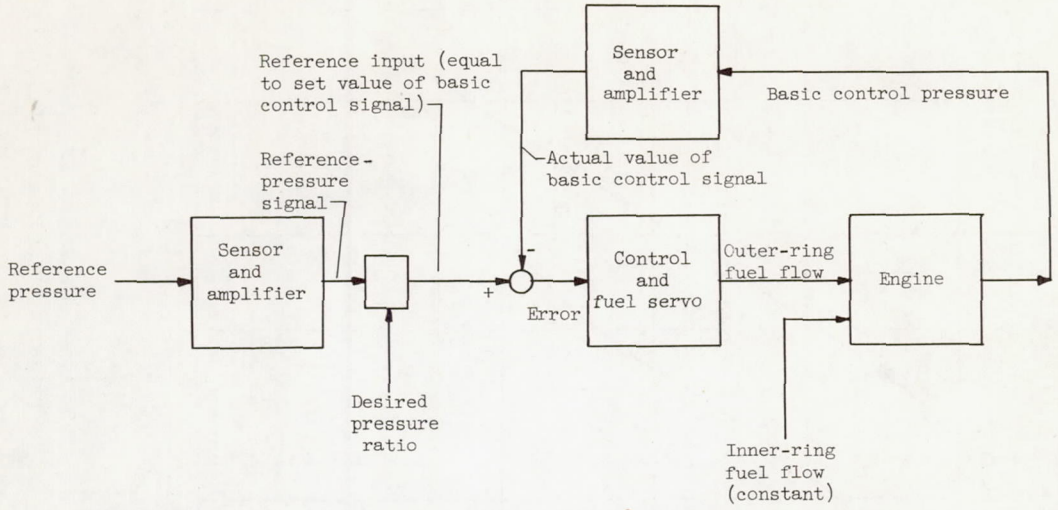

(a) Basic pressure-ratio control loop without limit loop.

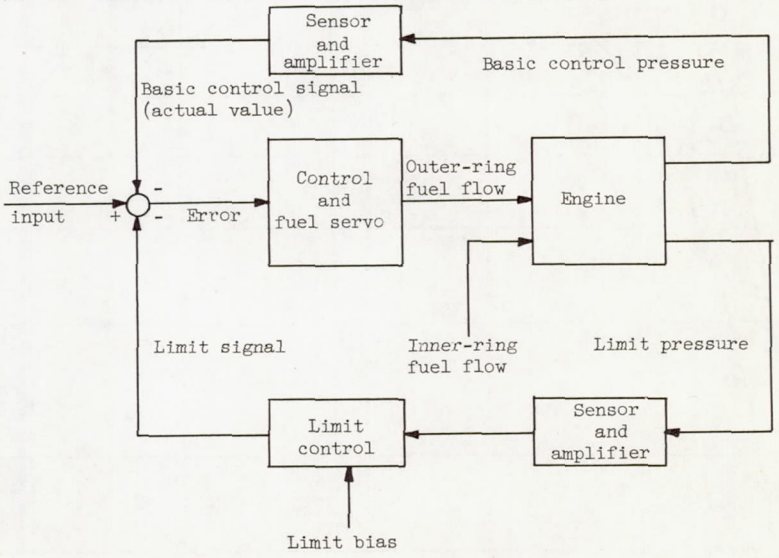

(b) Basic pressure-ratio control loop with limit loop.

Figure 8. - Simplified block diagram of control system.

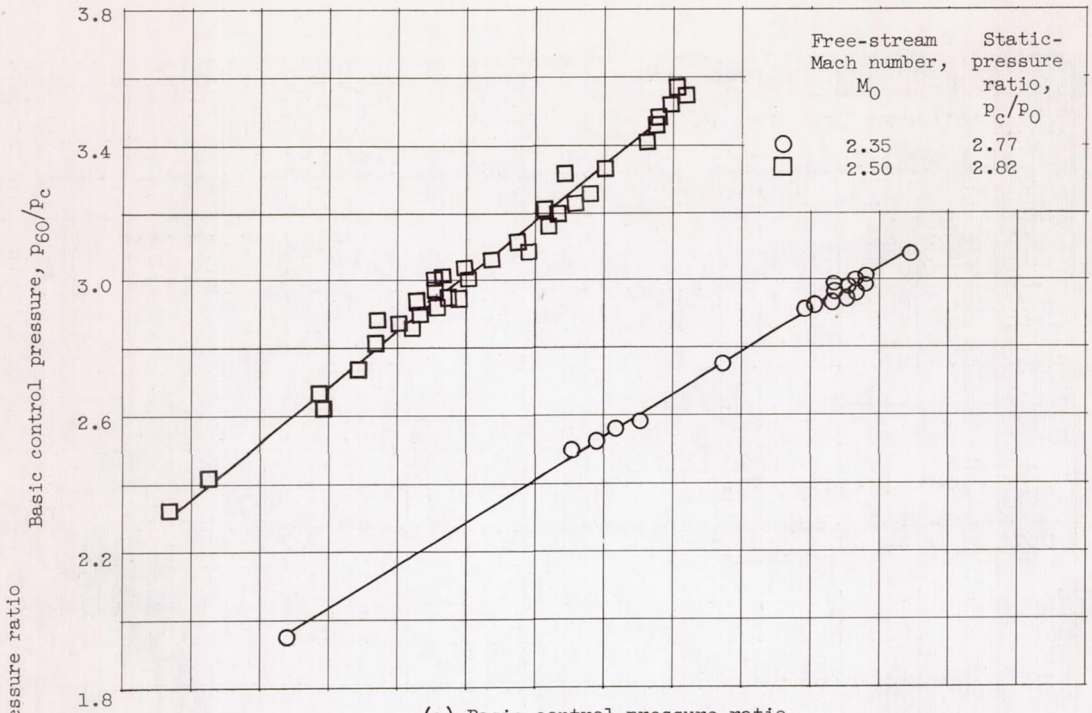

(a) Basic control pressure ratio.

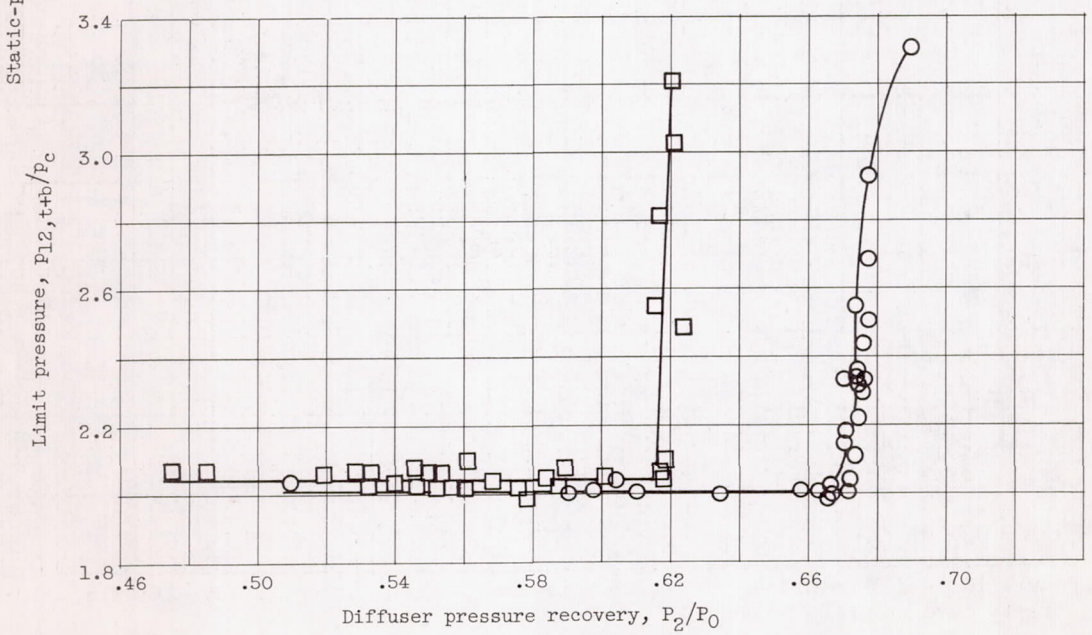

(b) Limit pressure ratio.

Figure 9. - Ratio of basic control and limit pressure to reference pressure as function of diffuser recovery at zero angle of attack.

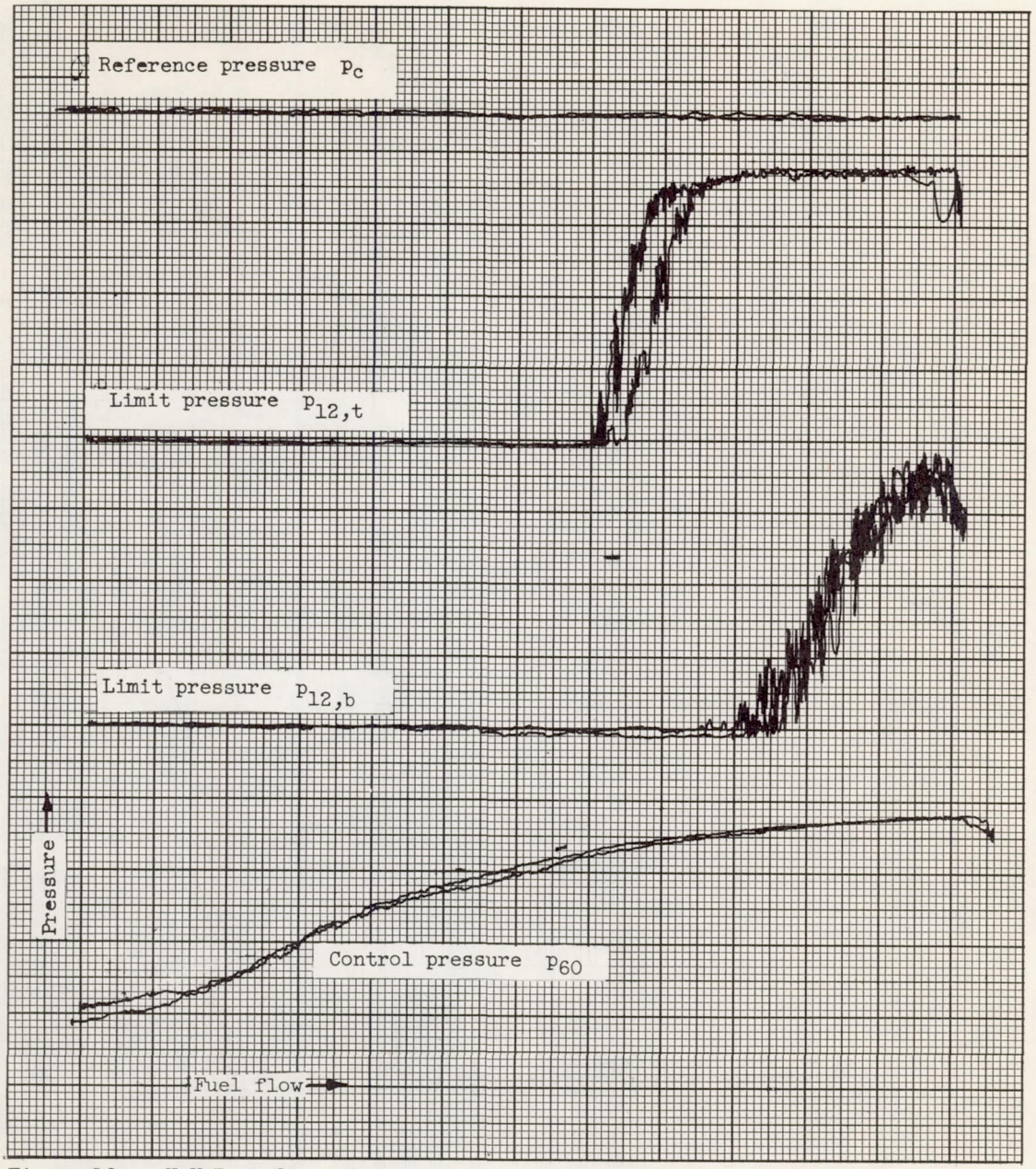

Figure 10. - X-Y Recording of engine pressures. Mach number, 2.35; altitude, 60,000 feet; zero angle of attack.

Free-stream Mach number, M_O	Altitude, h, ft	Free-stream static pressure, p_O lb/sq ft	Free-stream total pressure, P_O lb/sq ft	Inlet-air total temperature T, °F	Air flow, w_a lb/sec
2.35	50,000	242	3275	356	40.8
	60,000	151	2040		26.2
	65,000	119	1609		20.7
2.50	50,000	242	4138	413	47.3
	60,000	151	2578		29.5
	65,000	119	2025		23.0

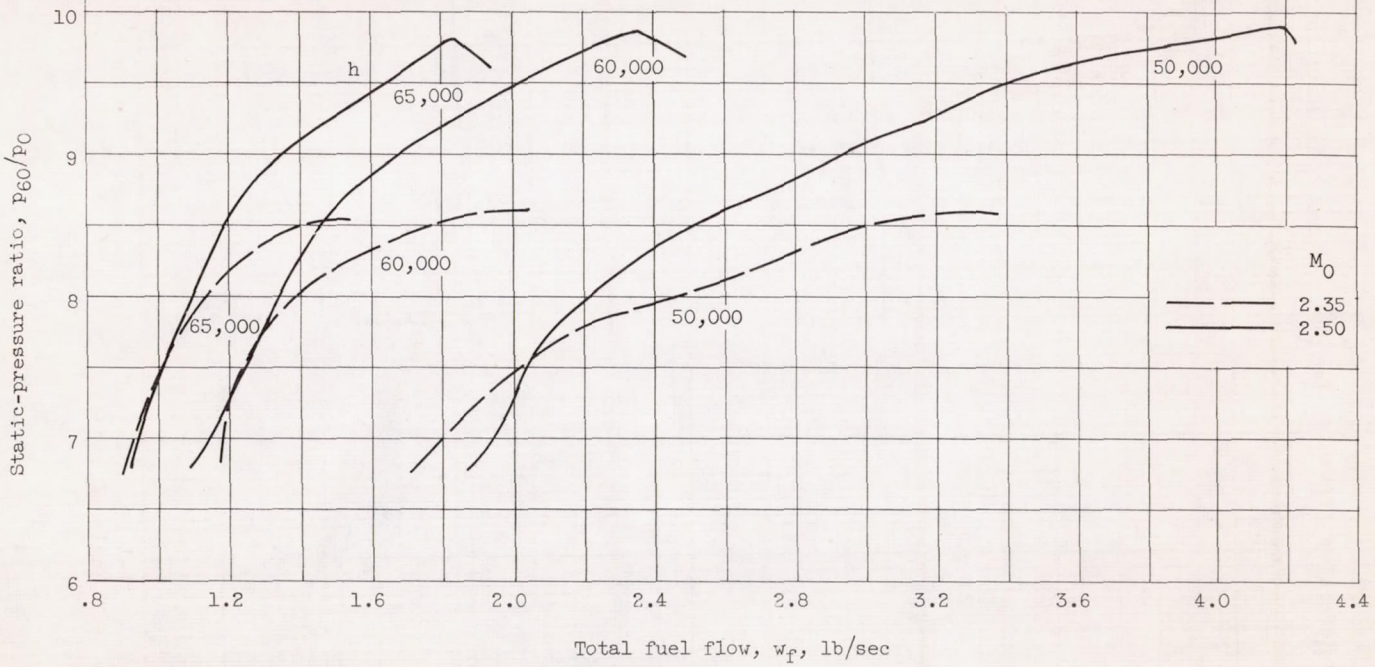

(a) Basic control pressure.

Figure 11. - Variation of diffuser static-pressure ratio with fuel flow at several flight conditions. Zero angle of attack.

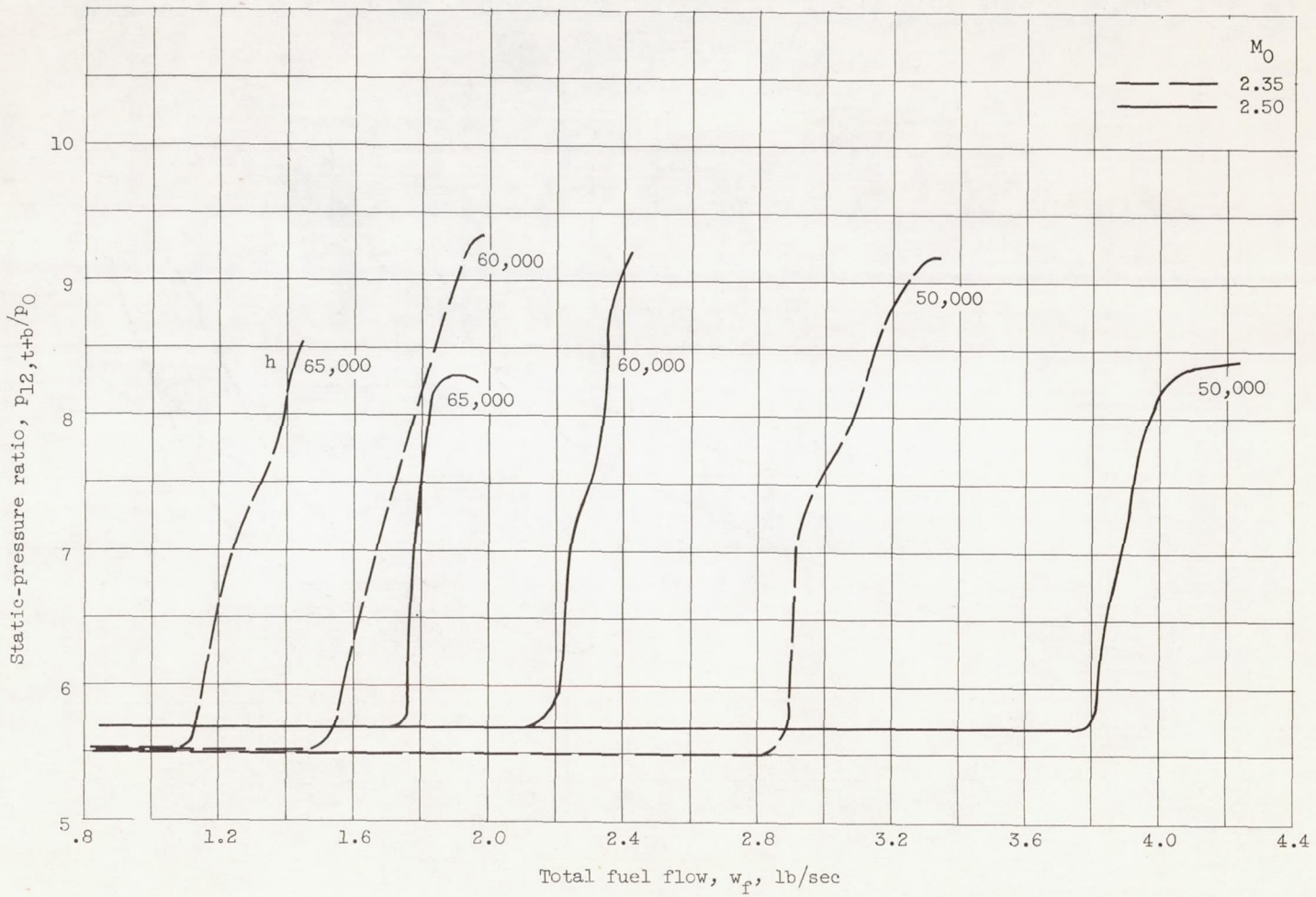

(b) Limit pressure.

Figure 11. - Concluded. Variation of diffuser static-pressure ratio with fuel flow at several flight conditions. Zero angle of attack.

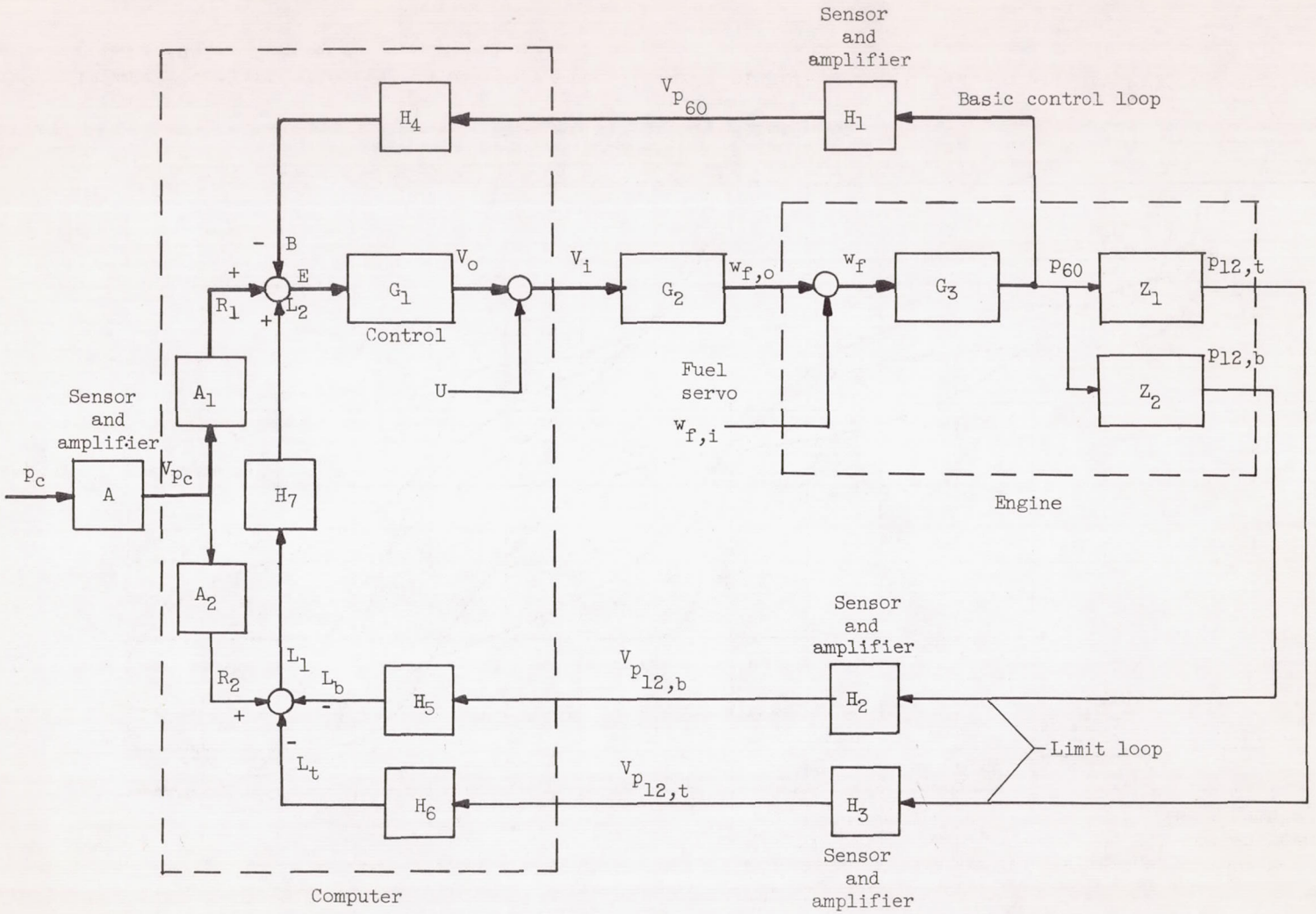

Figure 12. - Block diagram of pressure-ratio control with shock-positioning limit.

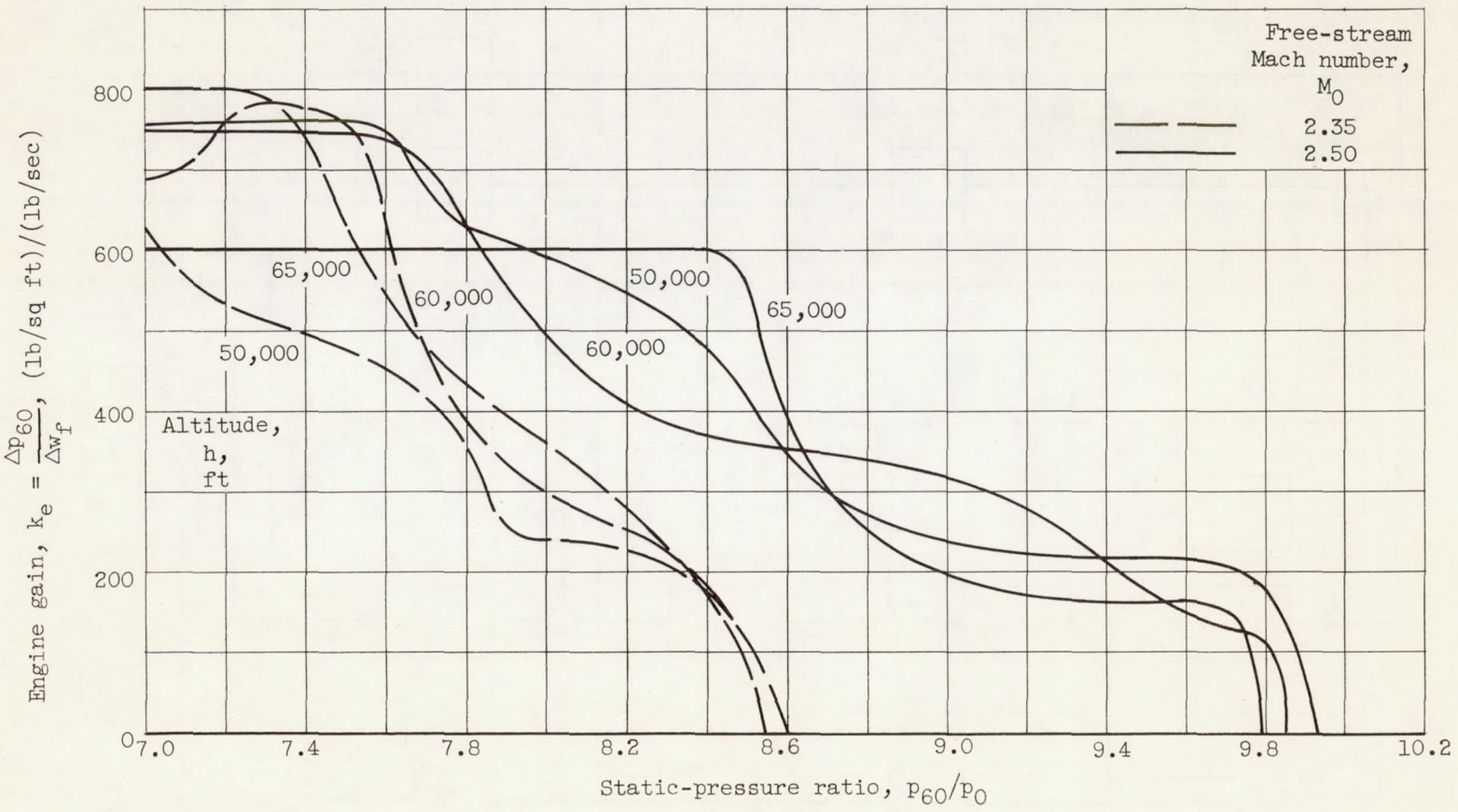

Figure 13. - Variation of engine gain with diffuser static-pressure ratio at several flight conditions. Zero angle of attack.

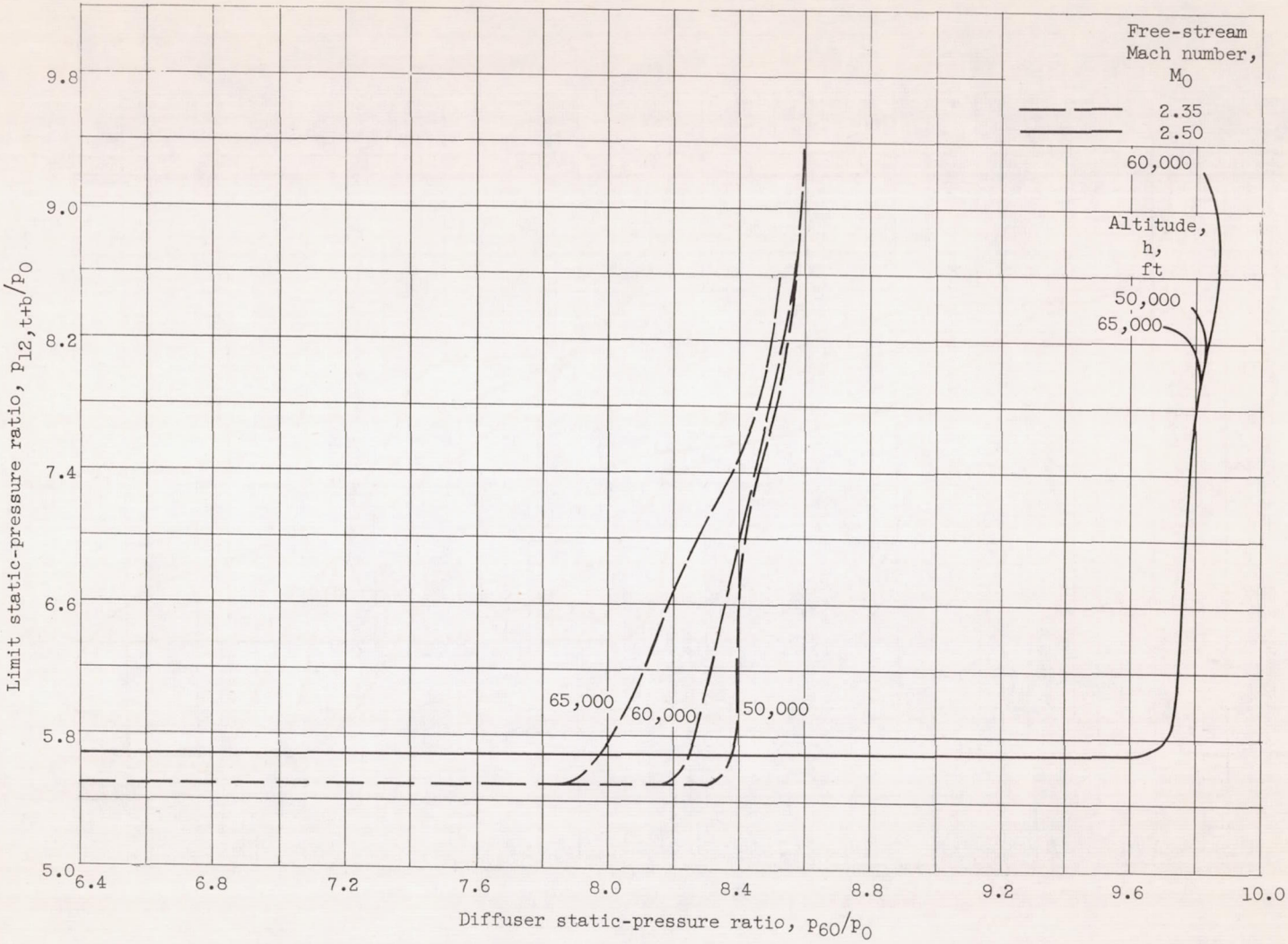

Figure 14. - Variation of limit-pressure ratio with basic control-pressure ratio at several flight conditions. Zero angle of attack.

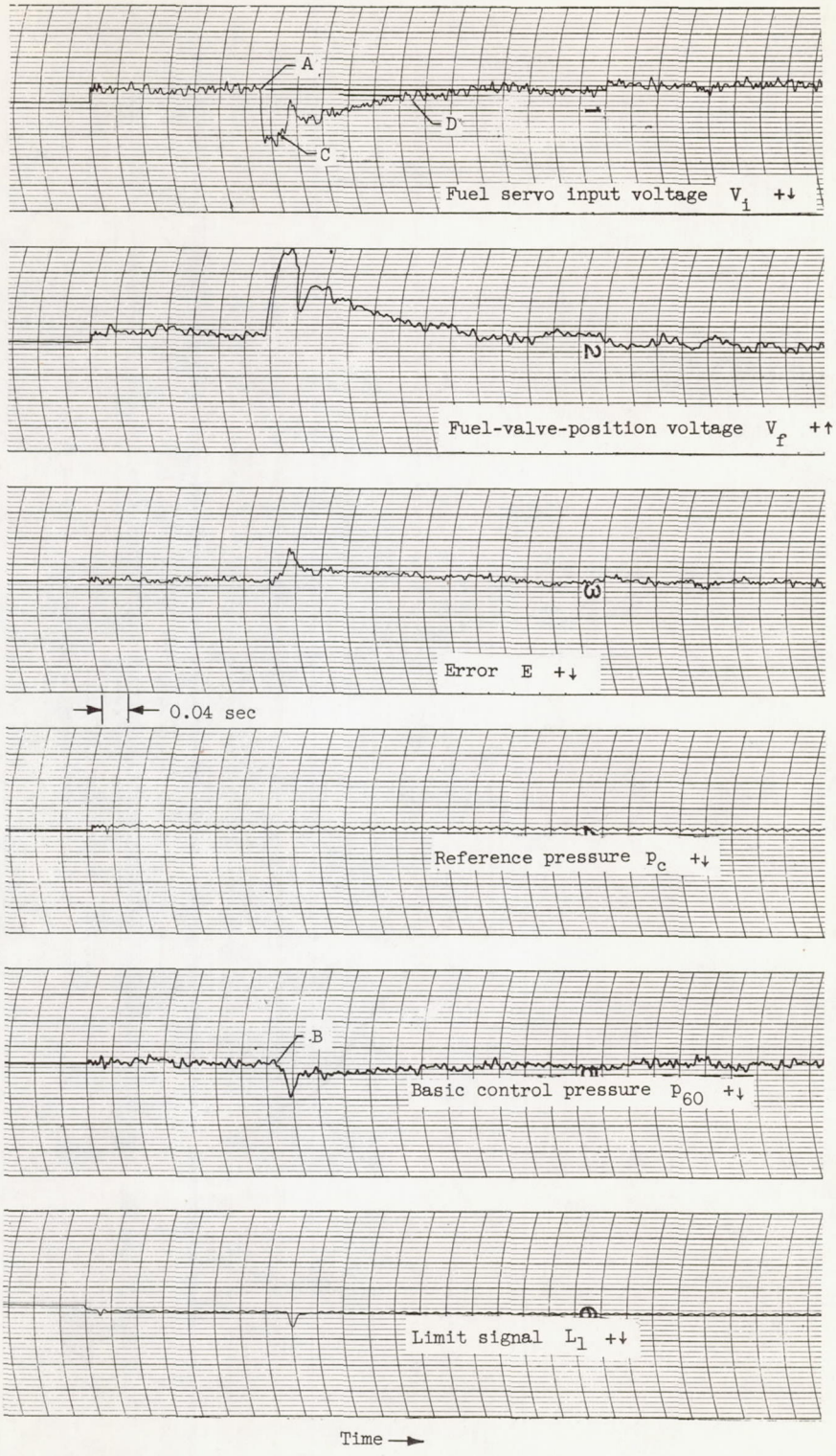

(a) Step increase.

Figure 15. - Oscillogram of basic loop response to step disturbance in fuel flow.

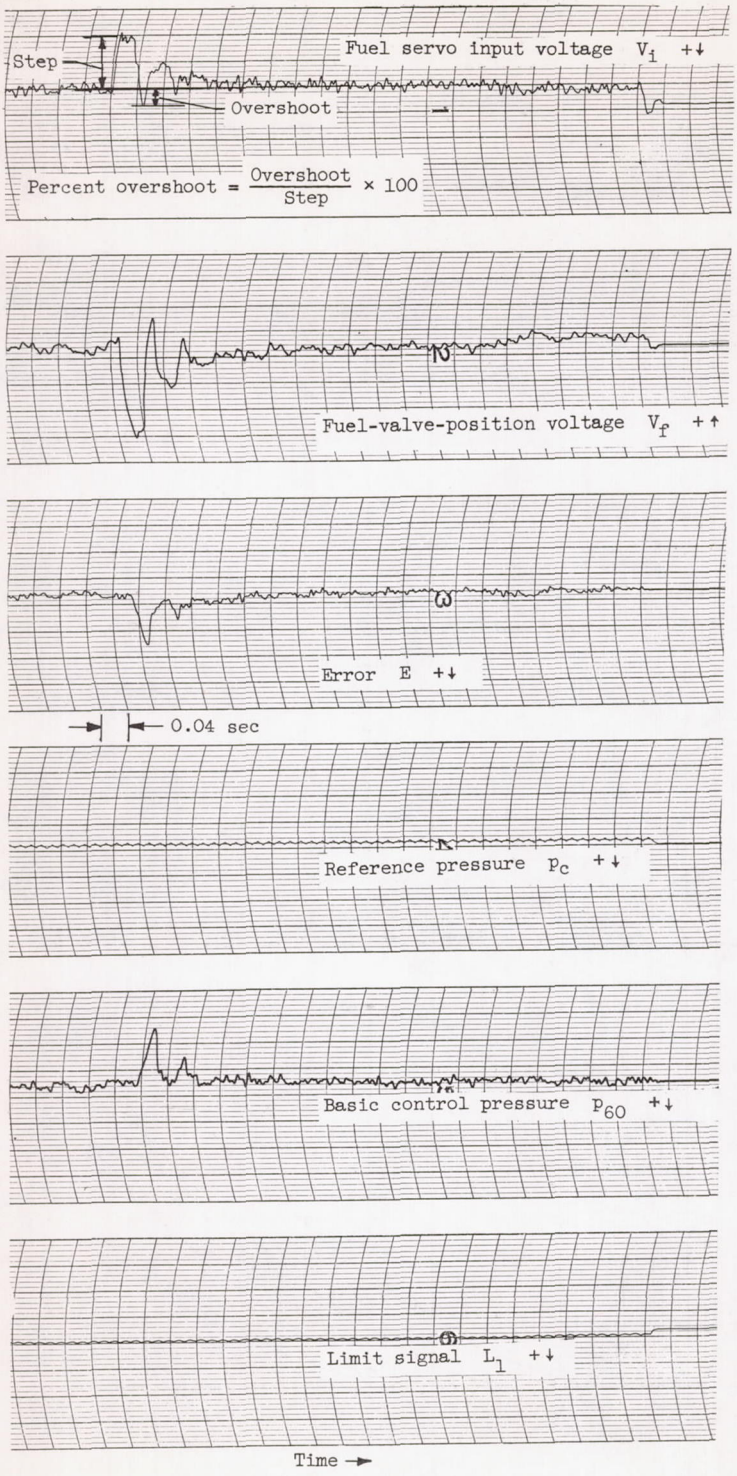

(b) Step decrease.

Figure 15. - Concluded. Oscillogram of basic loop response to step disturbance in fuel flow.

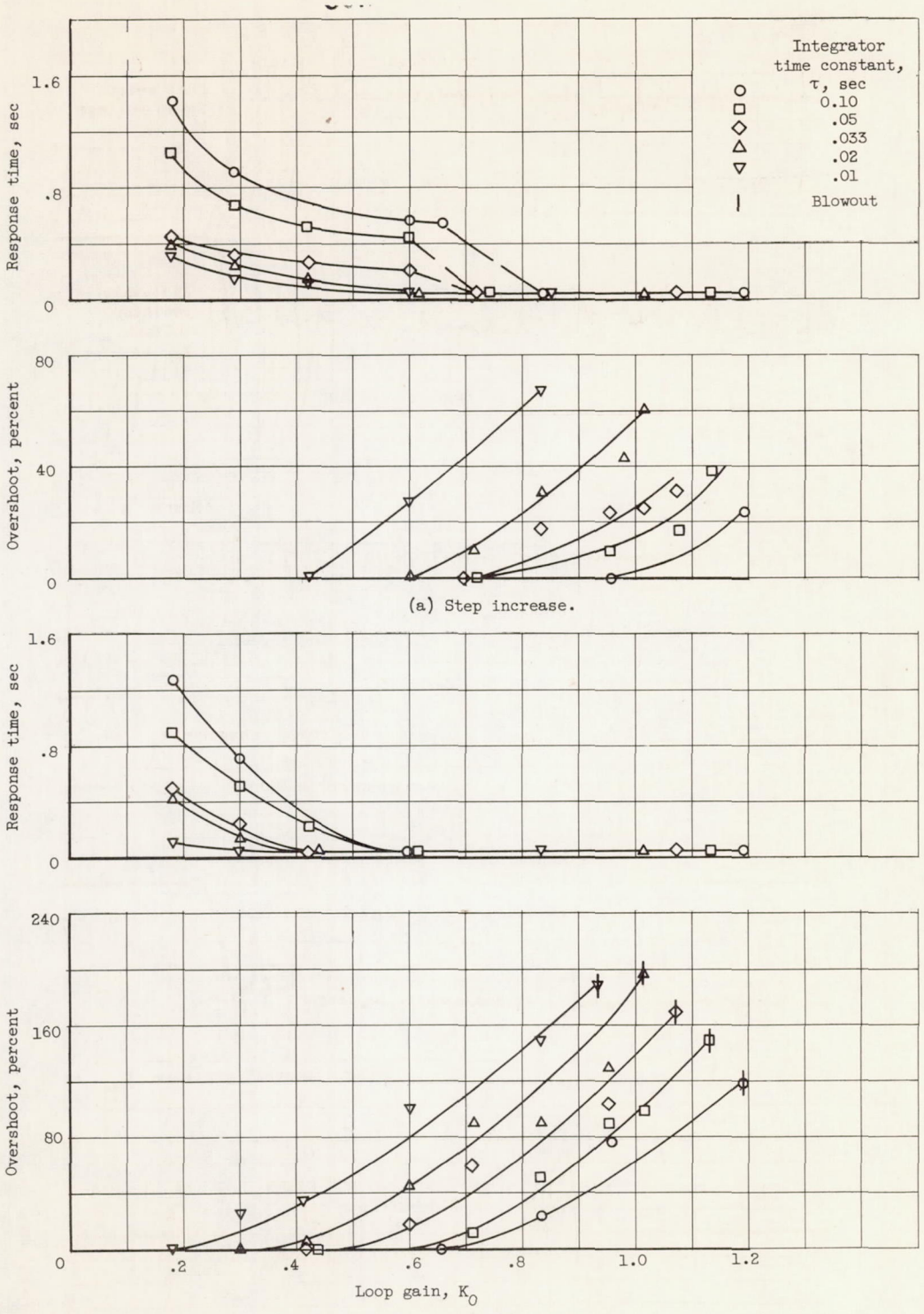

Figure 16. - Response of basic loop to step disturbance in fuel flow at Mach 2.35. Zero limit gain; altitude 60,000 feet; zero angle of attack; control pressure ratio P_{60}/P_0, 8.29; fuel flow step size, ±0.26 pound per second.

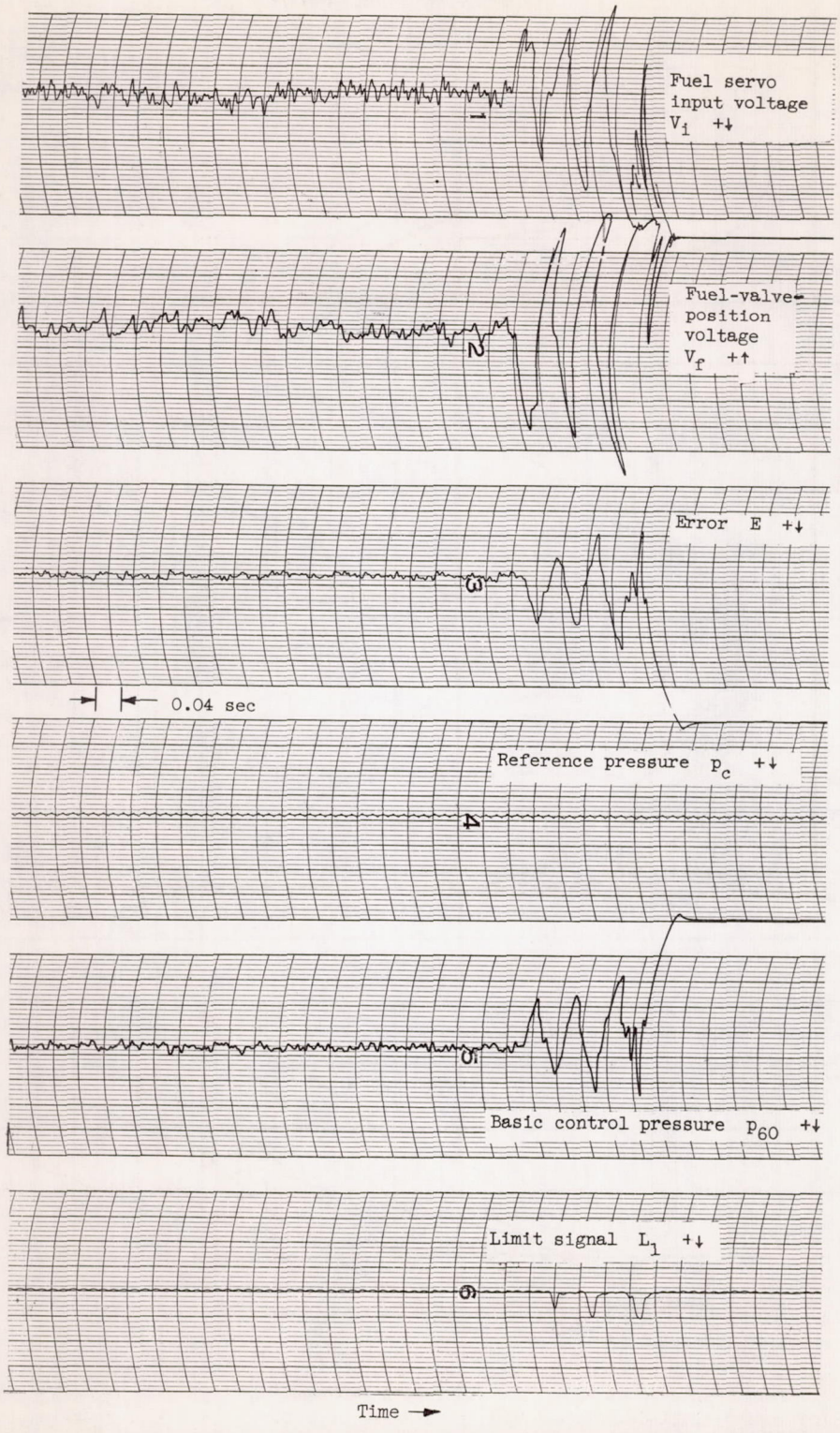

Figure 17. - Oscillogram of divergent oscillation resulting in blow-out following step decrease in fuel flow.

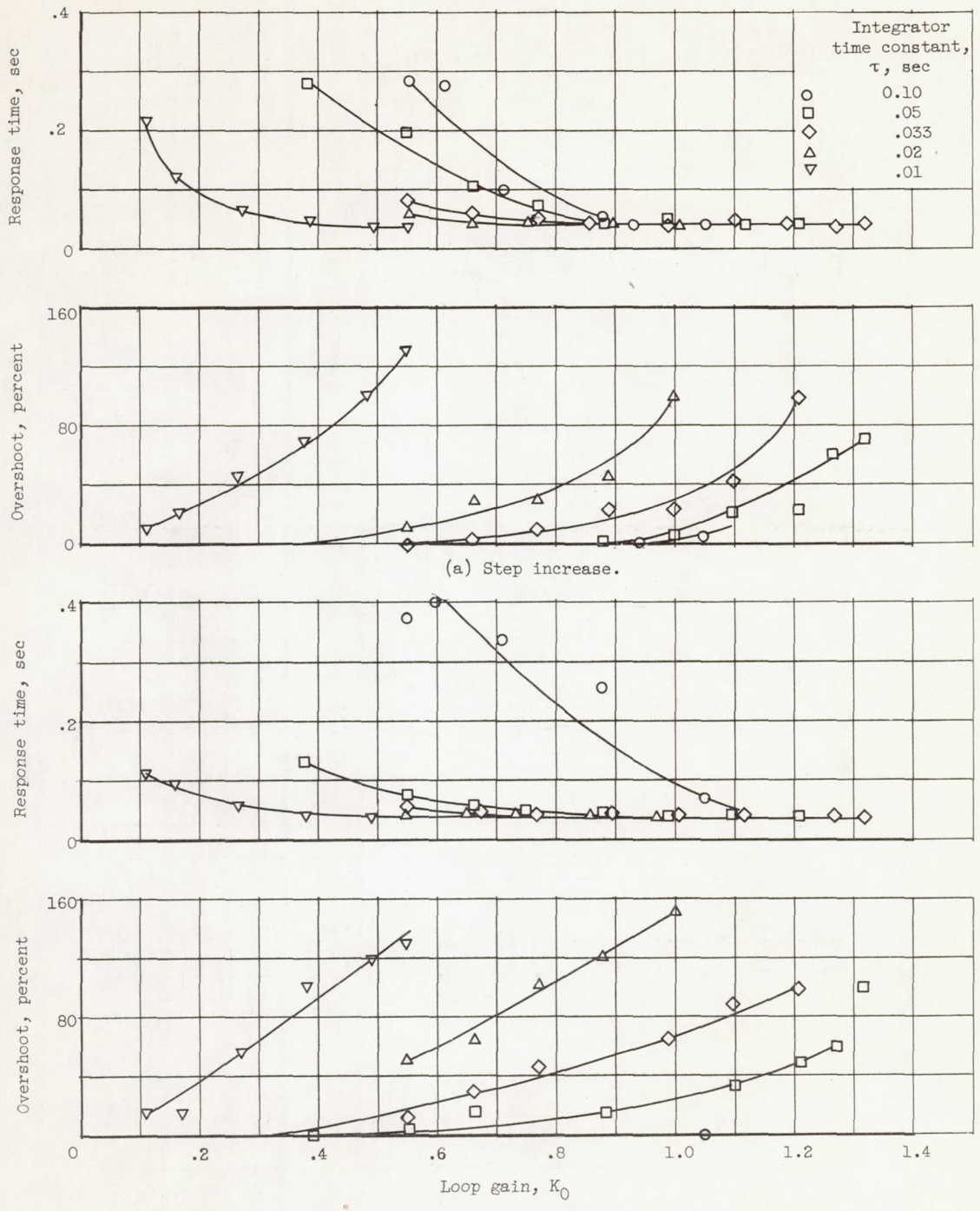

Figure 18. - Response of basic loop to step disturbance in fuel flow at Mach 2.50. Zero limit gain; altitude, 60,000 feet; zero angle of attack; control pressure ratio p_{60}/p_0, 8.33; fuel flow step size, ±0.291 pound per second.

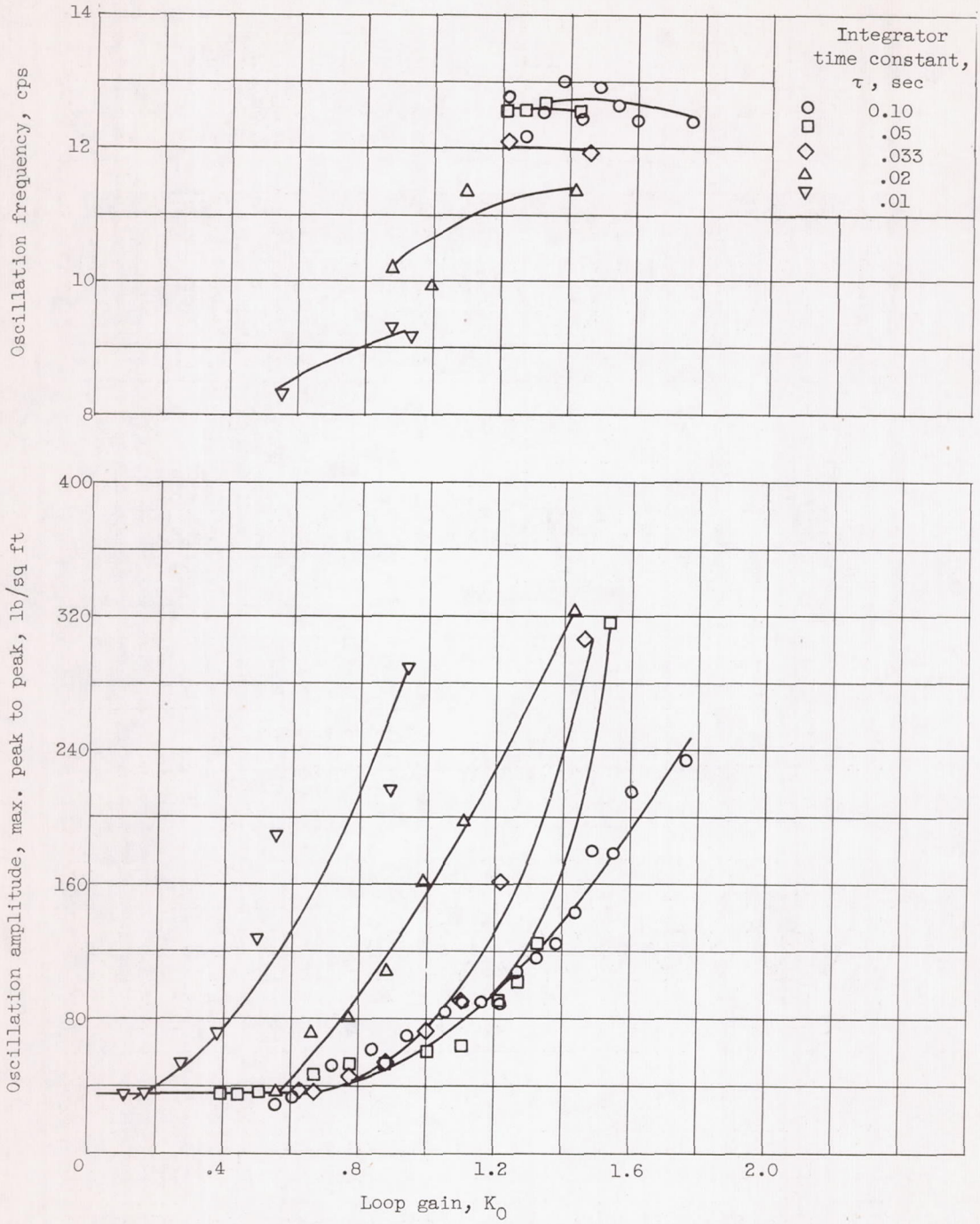

Figure 19. - Basic loop stability at Mach 2.50.

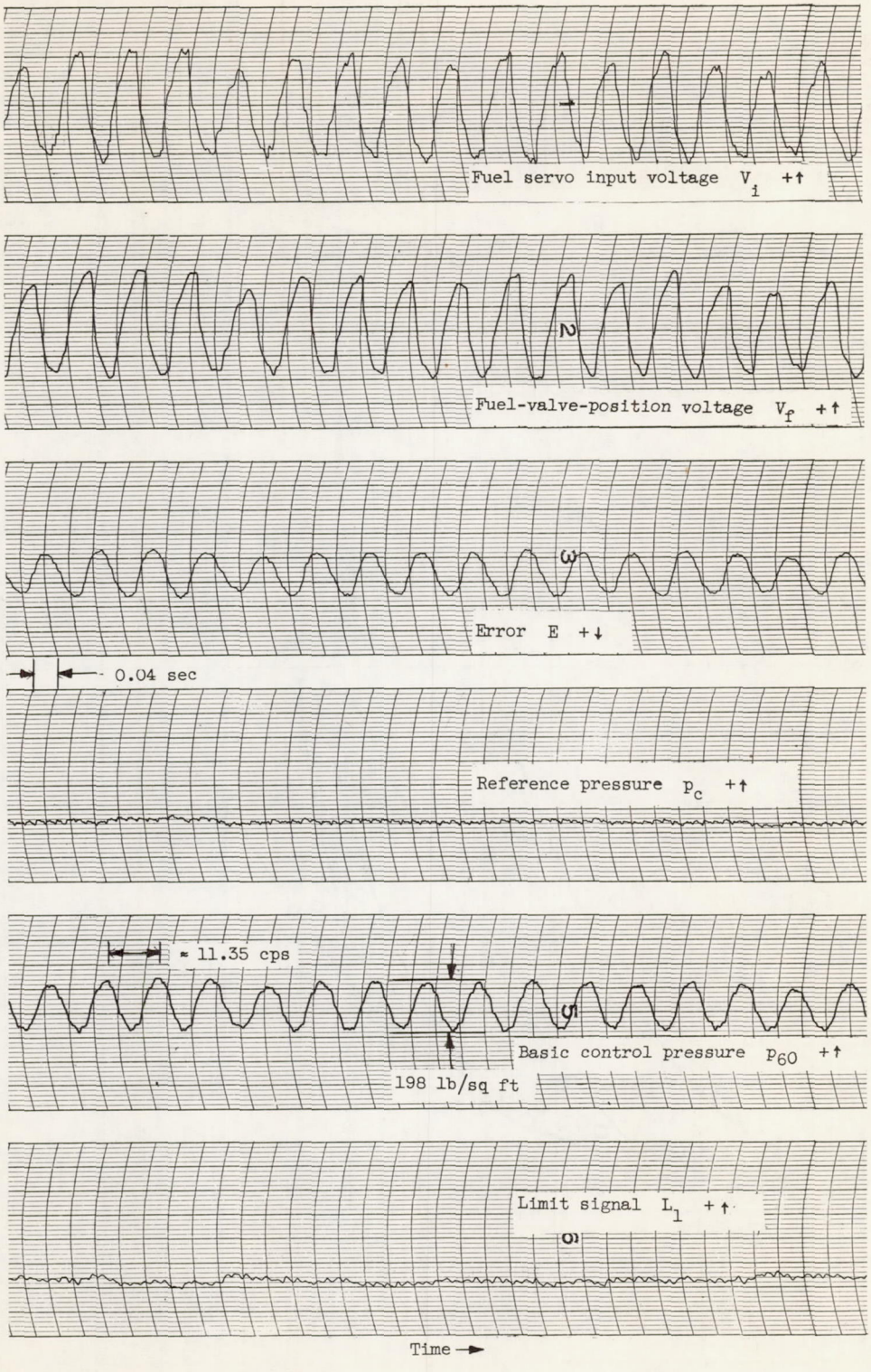

Figure 20. - Oscillogram of sustained oscillation at Mach 2.50. Loop gain, 1.10; integrator time constant, 0.02 second.

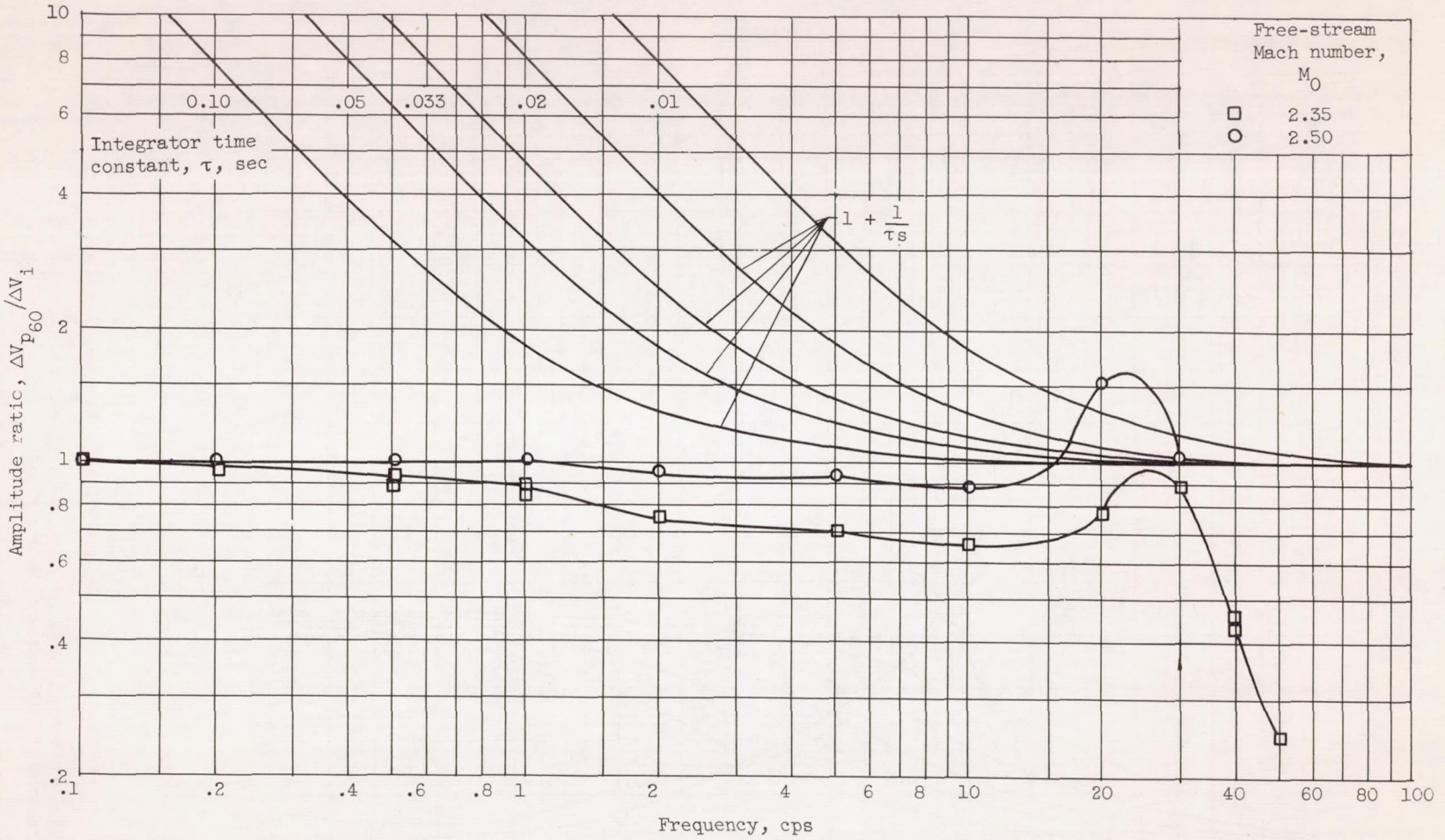

(a) Amplitude ratio.

Figure 21. - Open-loop frequency-response characteristics of basic control loop. Zero angle of attack; altitude, 60,000 feet.

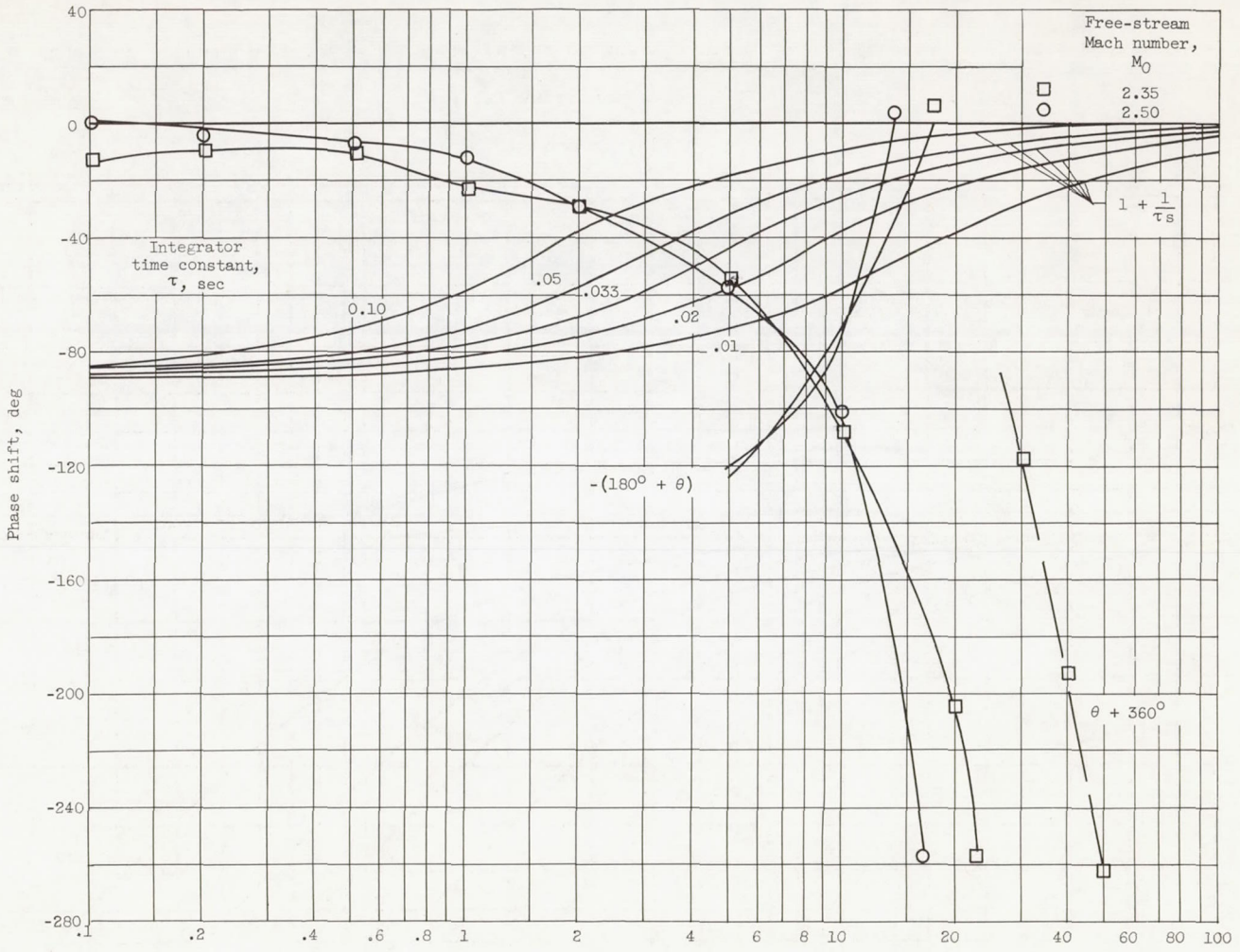

(b) Phase shift

Figure 21. - Concluded. Open-loop frequency-response characteristics of basic control loop. Zero angle of attack; altitude, 60,000 feet.

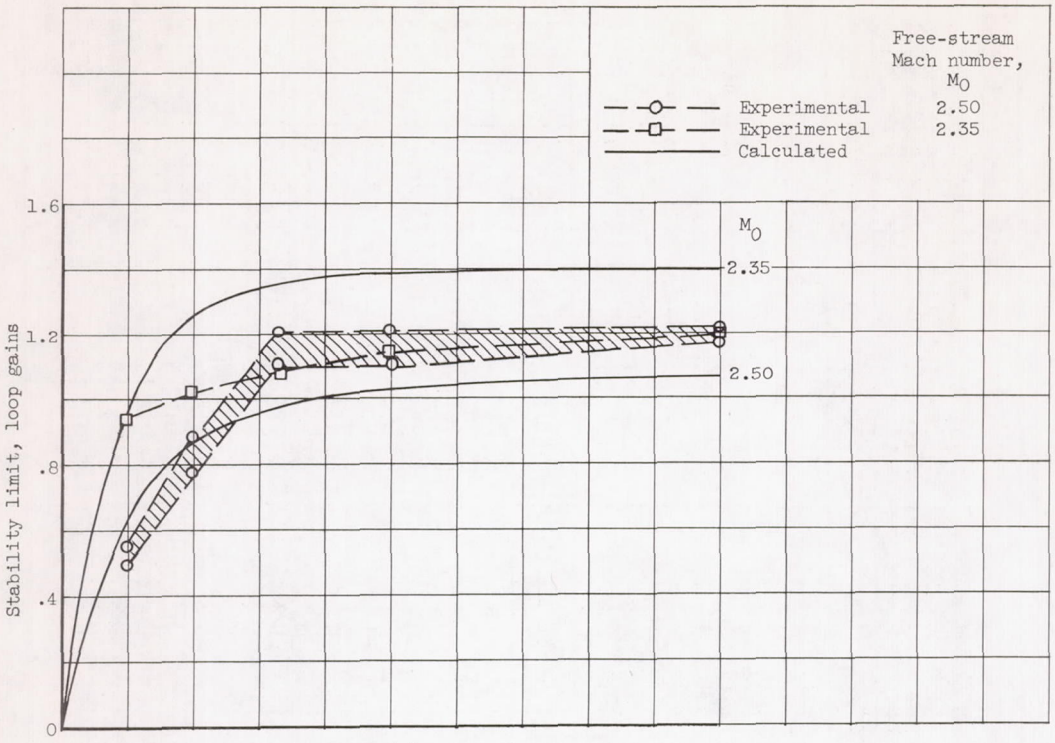

(a) Loop gains for instability.

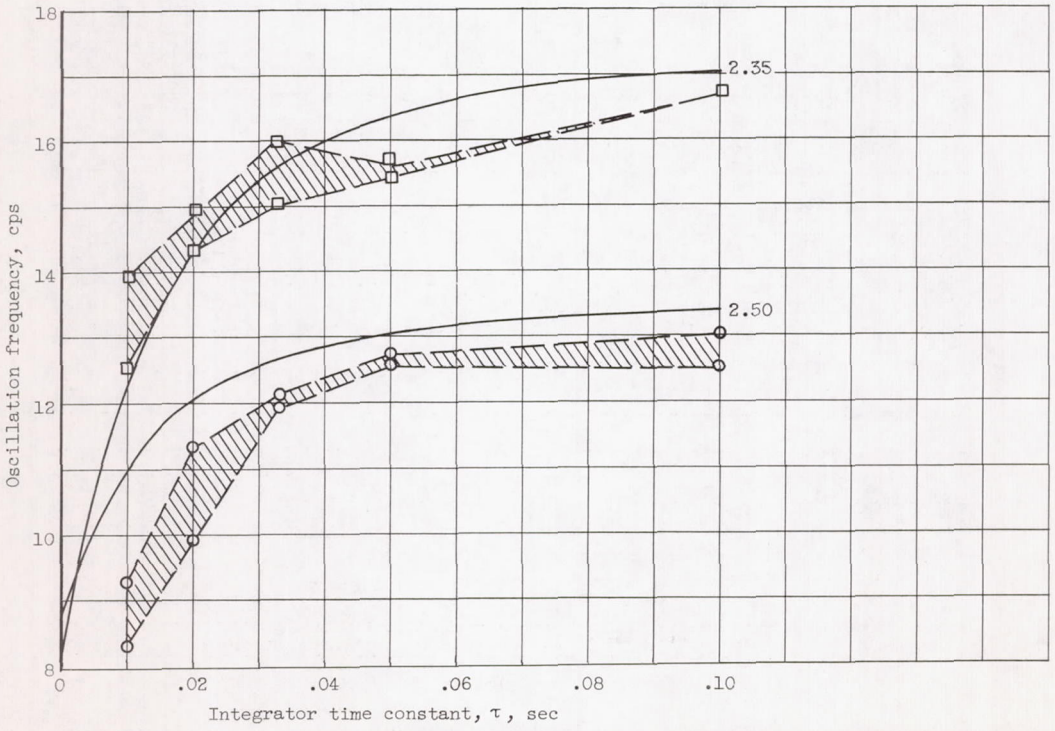

(b) Frequency of oscillation at instability.

Figure 22. - Stability limits of control system as function of integrator time constant.

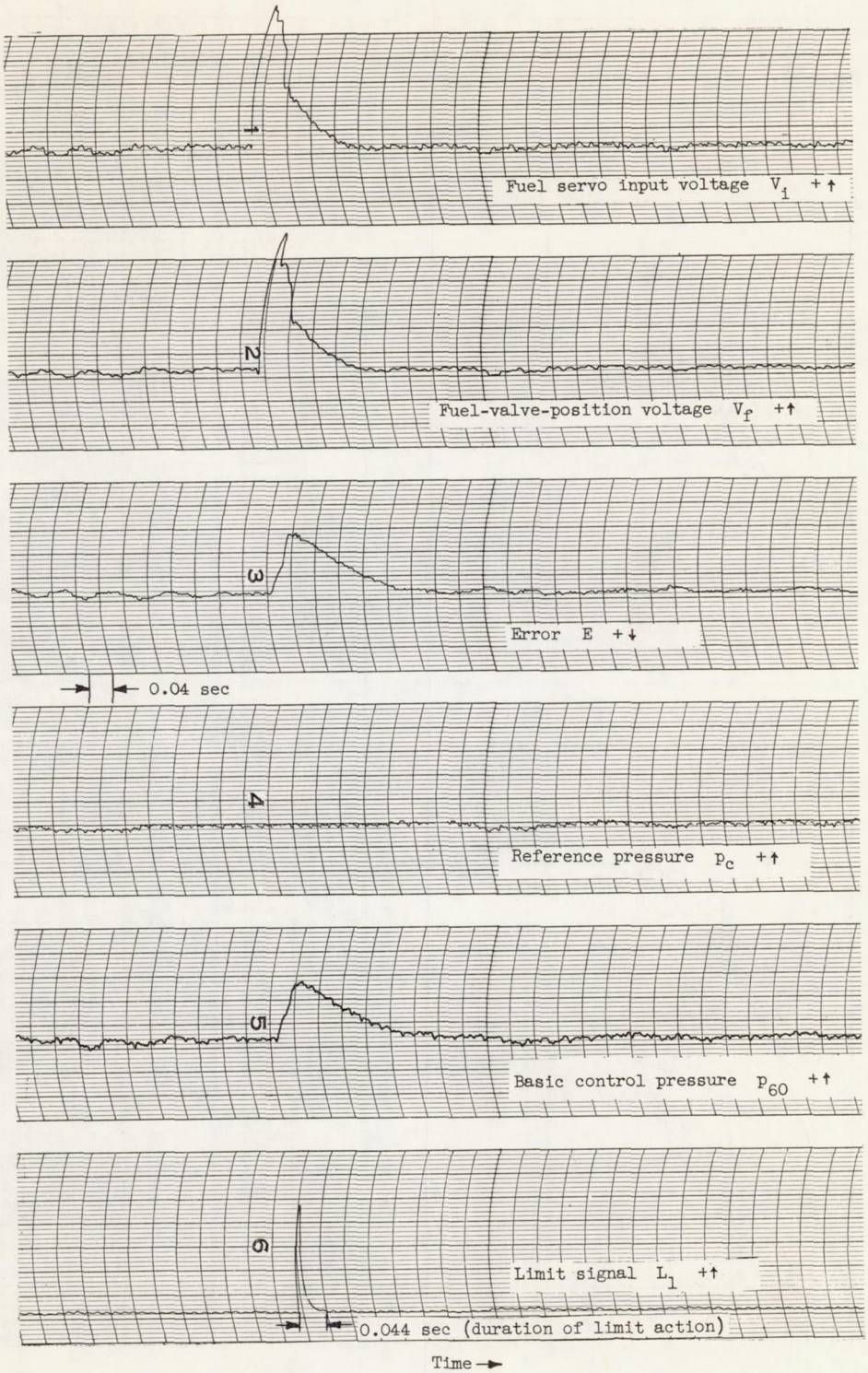

(a) Limit gain, 0.

Figure 23. - Oscillogram of system response to step disturbance at various limit gains.

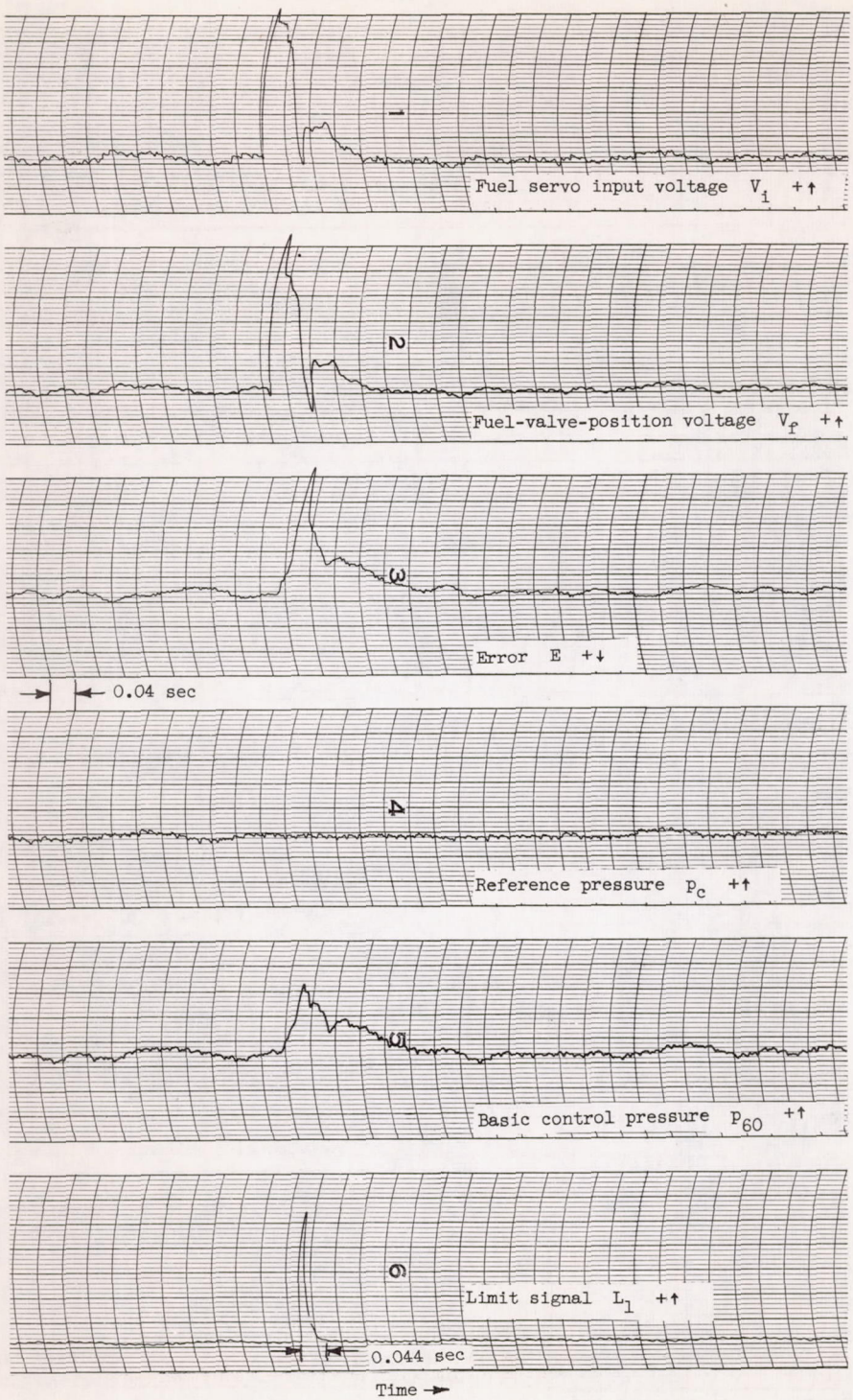

(b) Limit gain, Q.357.

Figure 23. - Continued. Oscillogram of system response to step disturbance at various limit gains.

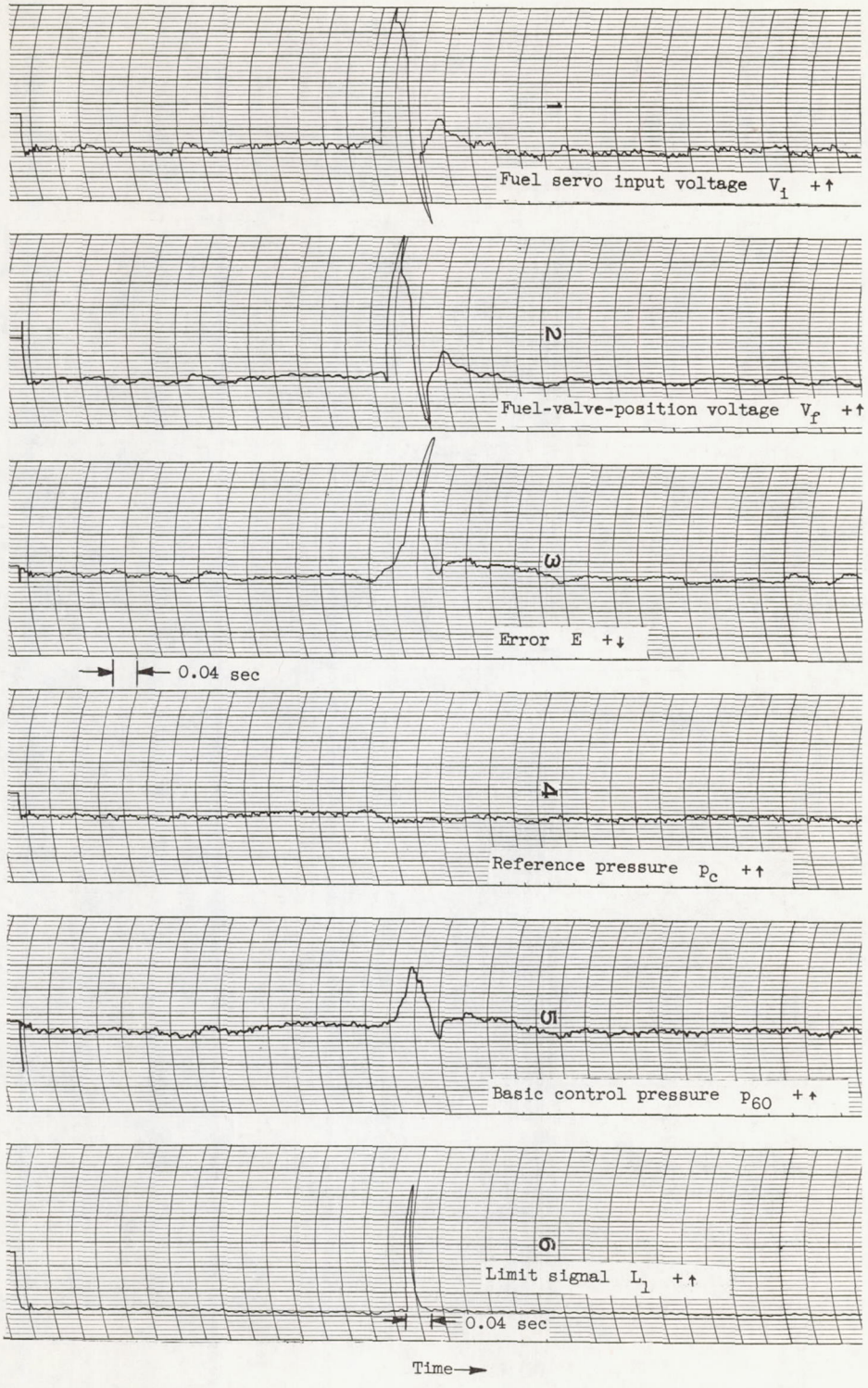

(c) Limit gain, 0.663.

Figure 23. - Concluded. Oscillogram of system response to step disturbance at various limit gains.

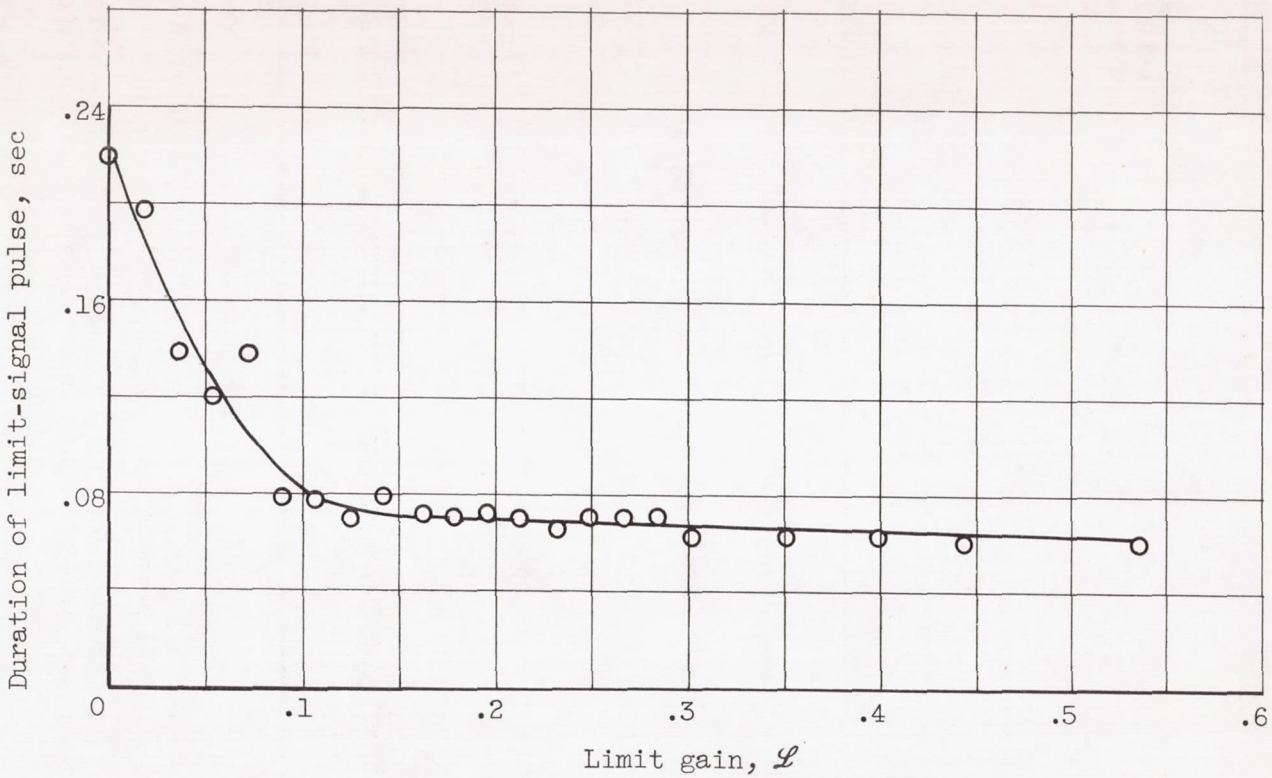

Figure 24. - Duration of limit-signal pulse during system response to step disturbance in fuel flow for operation at 97 percent of maximum diffuser recovery. Mach number, 2.35; altitude, 60,000 feet; zero angle of attack.

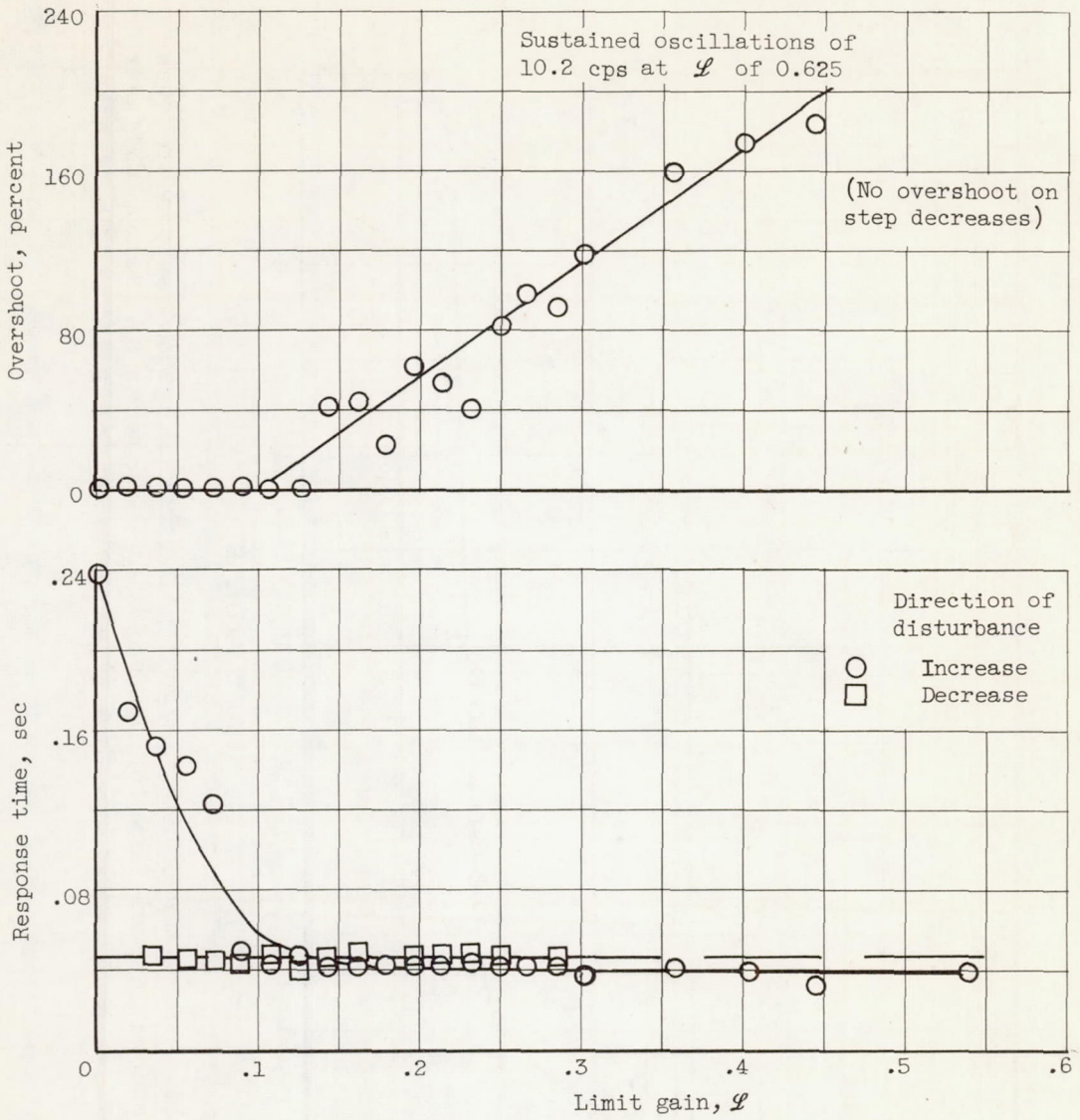

(a) Mach number, 2.35; loop gain, 0.503; fuel flow step size, ±0.26 pound per second; control pressure ratio p_{60}/p_0, 8.21.

Figure 25. - System response to step disturbance in fuel flow. Altitude, 60,000 feet; zero angle of attack; integrator time constant, 0.04 second.

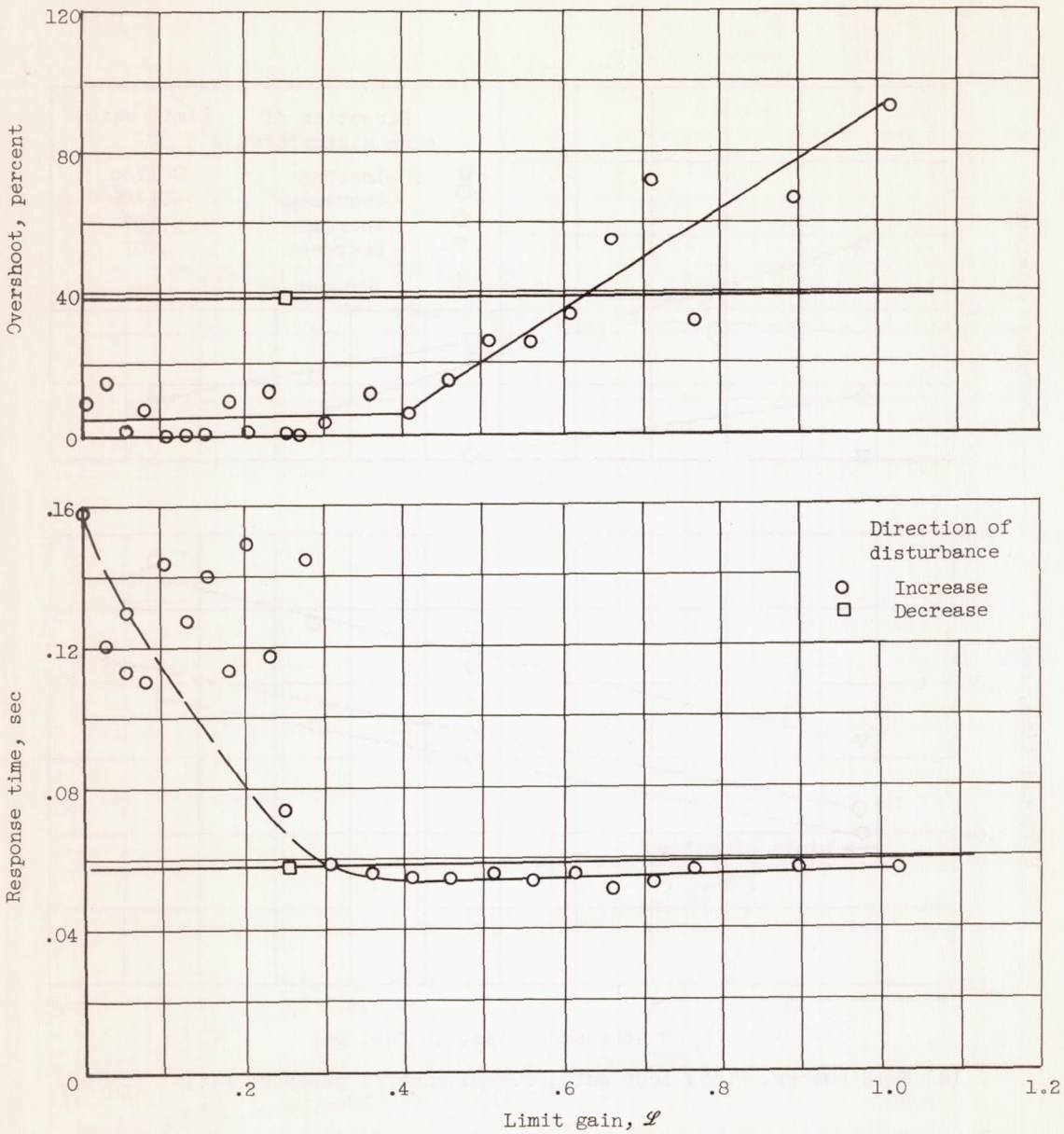

(b) Mach number, 2.50; loop gain, 0.848; fuel flow step size, $\pm$1.165 pounds per second; control pressure ratio p_{60}/p_0, 8.19

Figure 25. - Concluded. System response to step disturbance in fuel flow. Altitude, 60,000 feet; zero angle of attack; integrator time constant, 0.04 second.

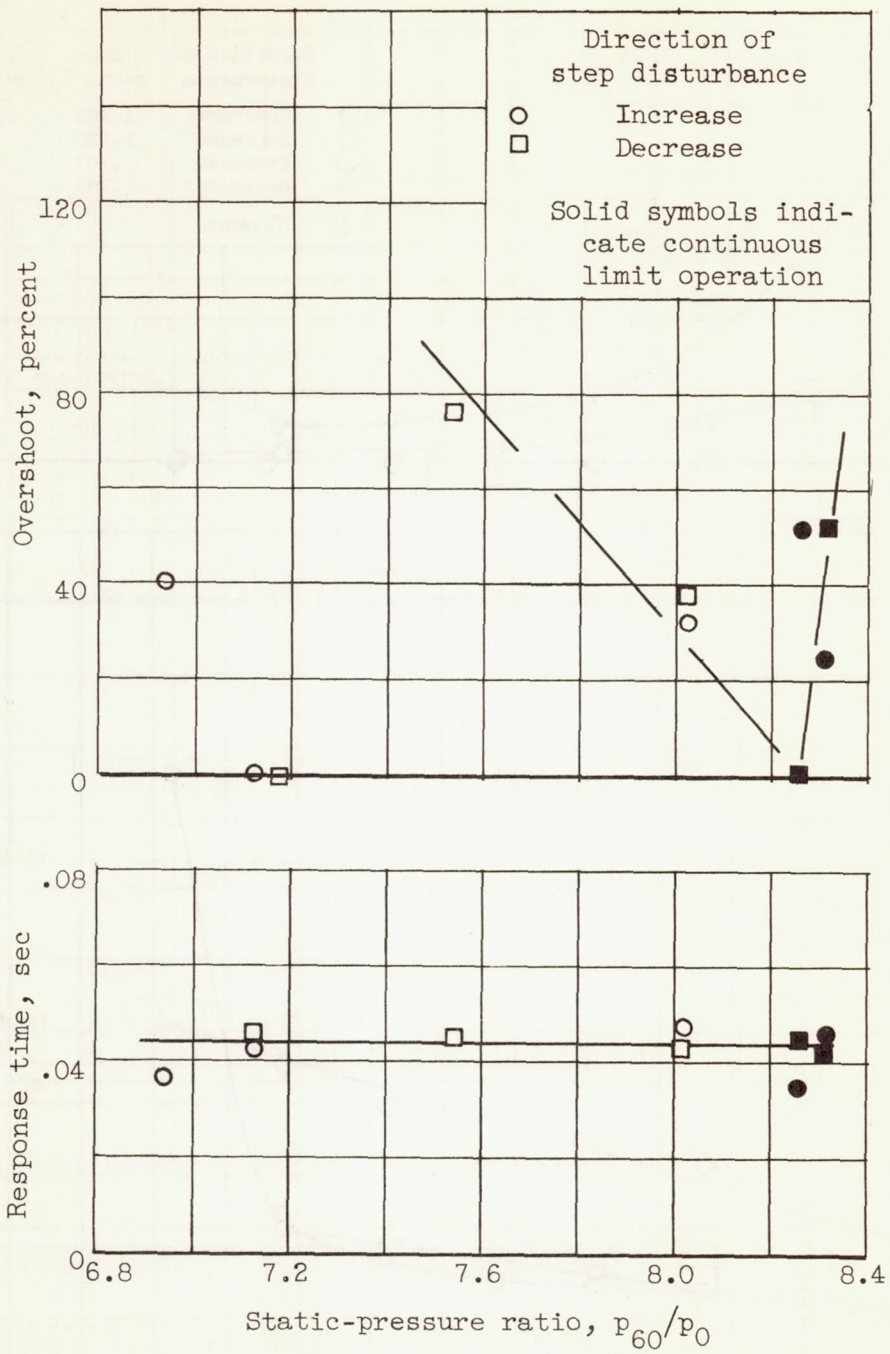

(a) Mach number, 2.35; loop gain, 0.00201 times engine gain; fuel flow step size, ±0.26 pound per second.

Figure 27. - System response at various diffuser pressure ratios. Altitude, 60,000 feet; zero angle of attack; limit gain, 0.1785; integrator time constant, 0.04 second.

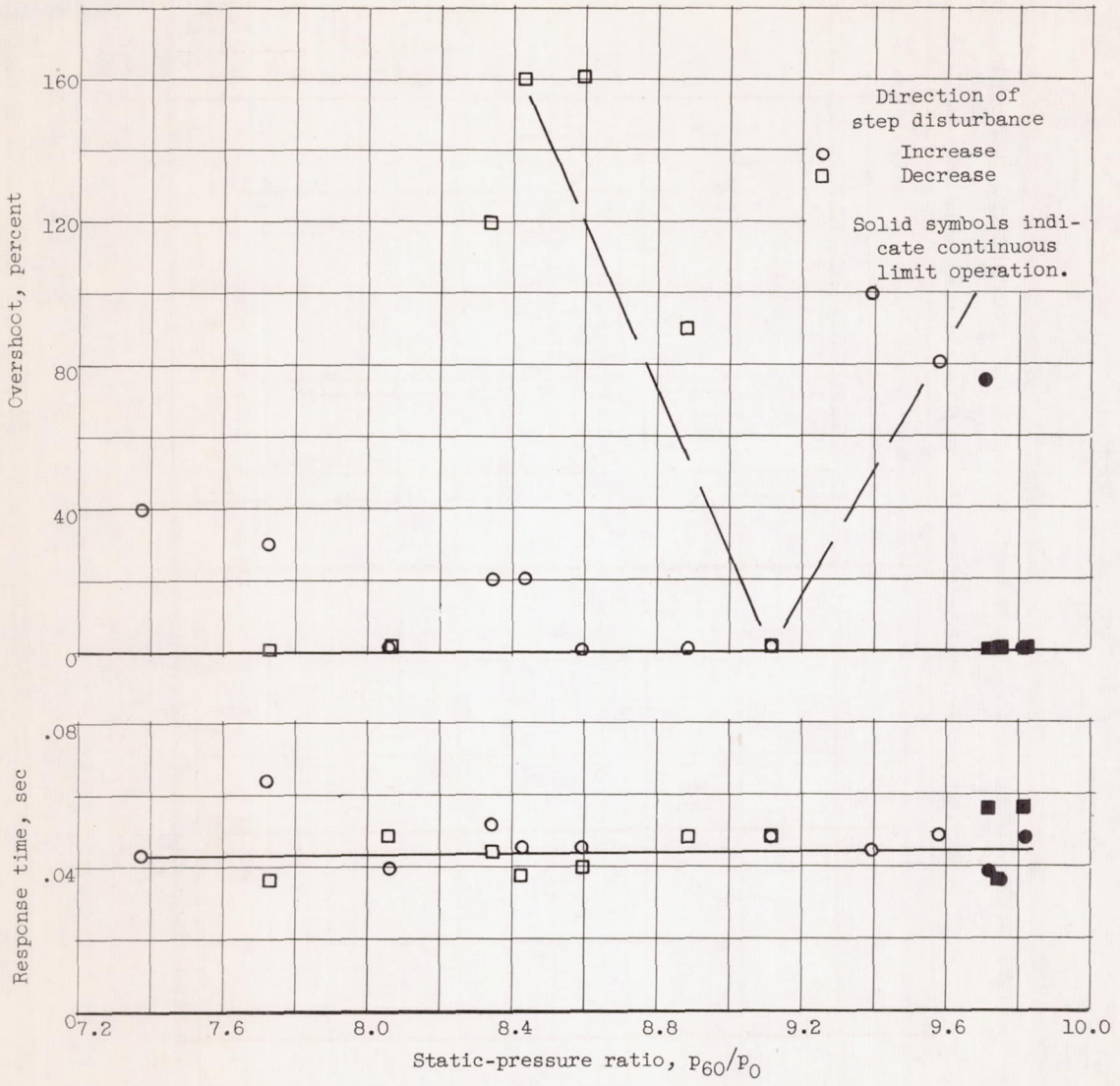

(b) Mach number, 2.50; loop gain, 0.00295 times engine gain; fuel flow step size, ±0.2915 pound per second.

Figure 27. - Concluded. System response at various diffuser pressure ratios. Altitude, 60,000 feet; zero angle of attack; limit gain, 0.1785; integrator time constant, 0.04 second.

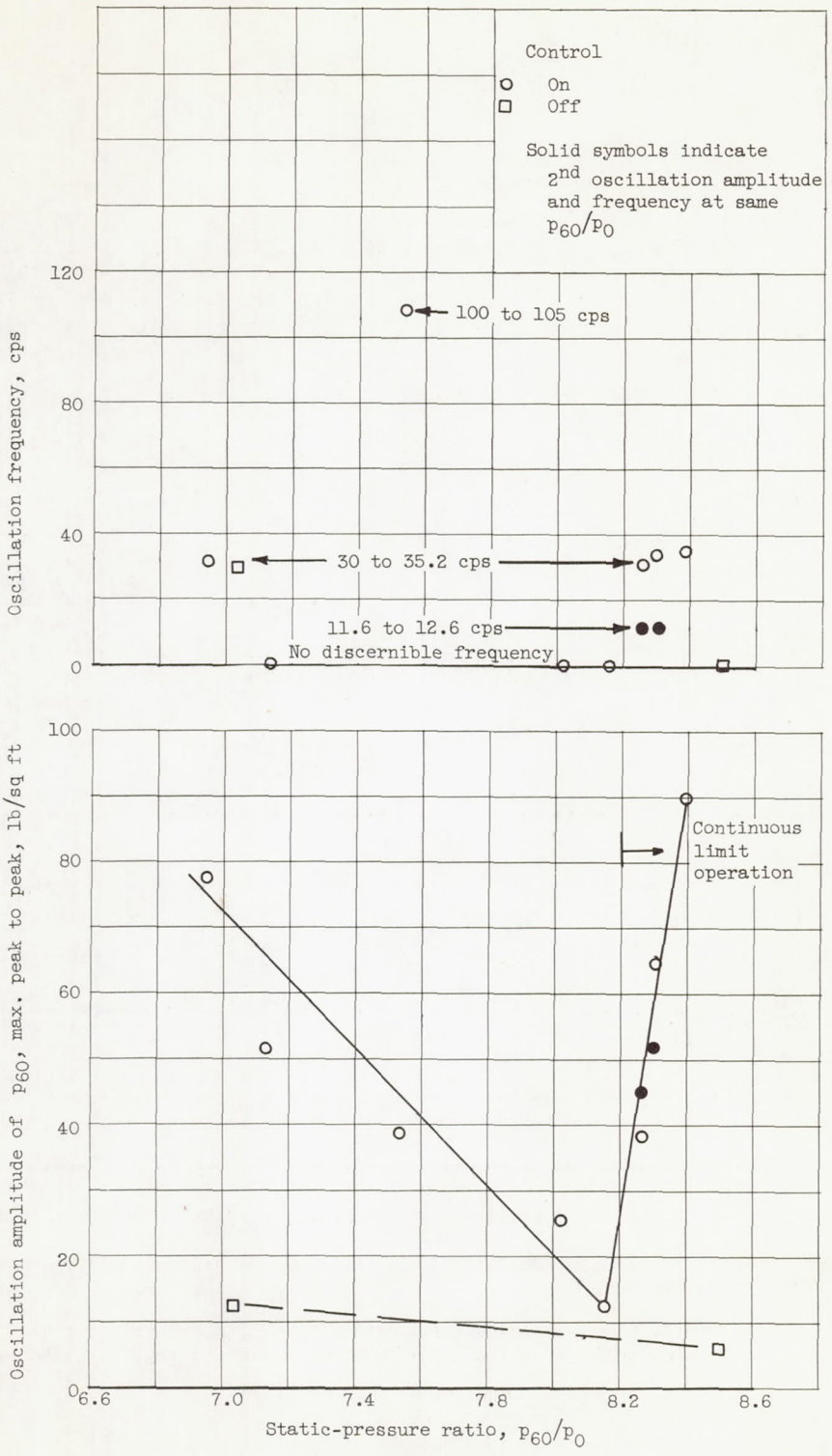

(a) Mach number, 2.35.

Figure 28. - System stability at various pressure ratios.

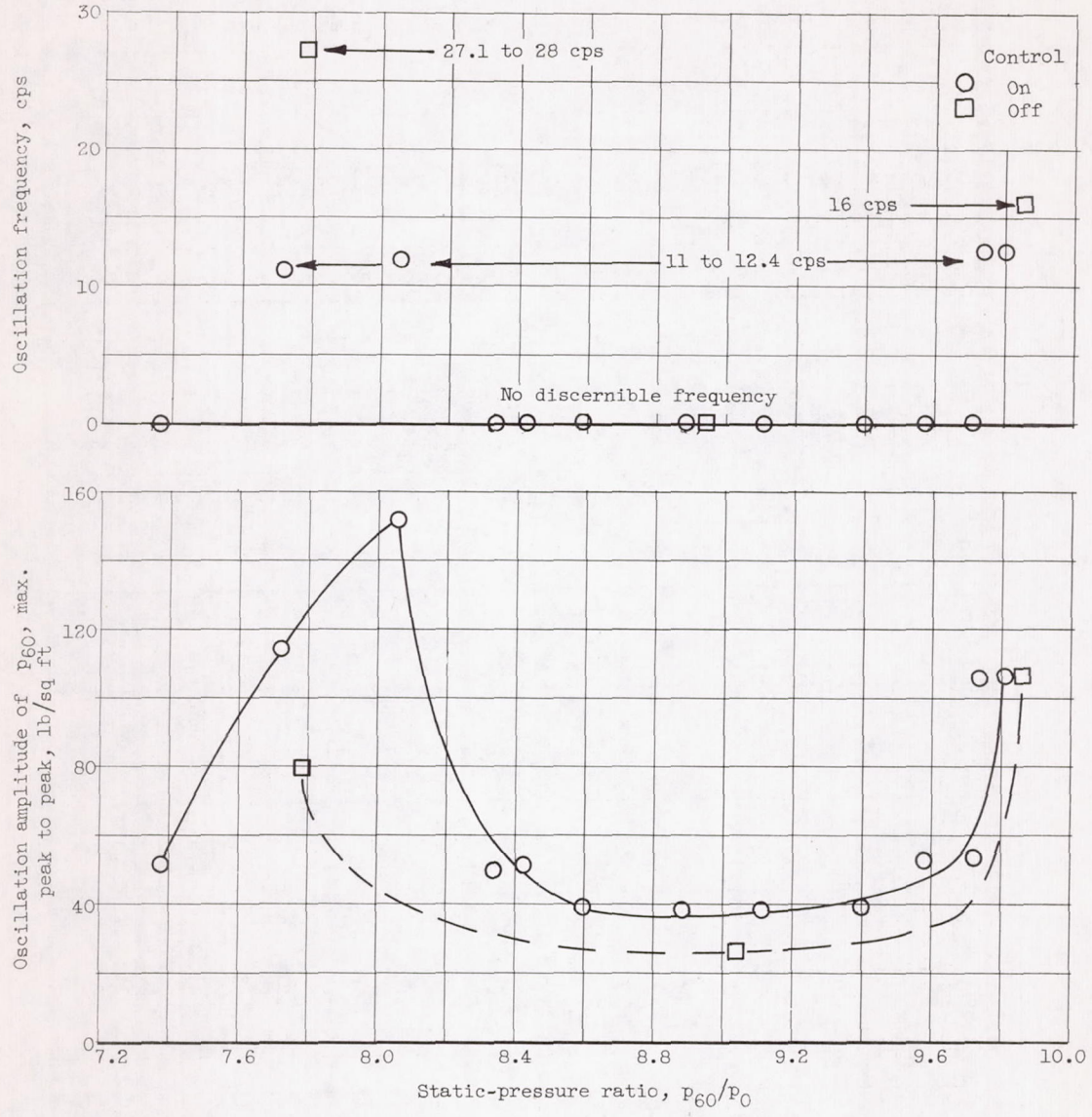

(b) Mach number, 2.50.

Figure 28. - Concluded. System stability at various pressure ratios.

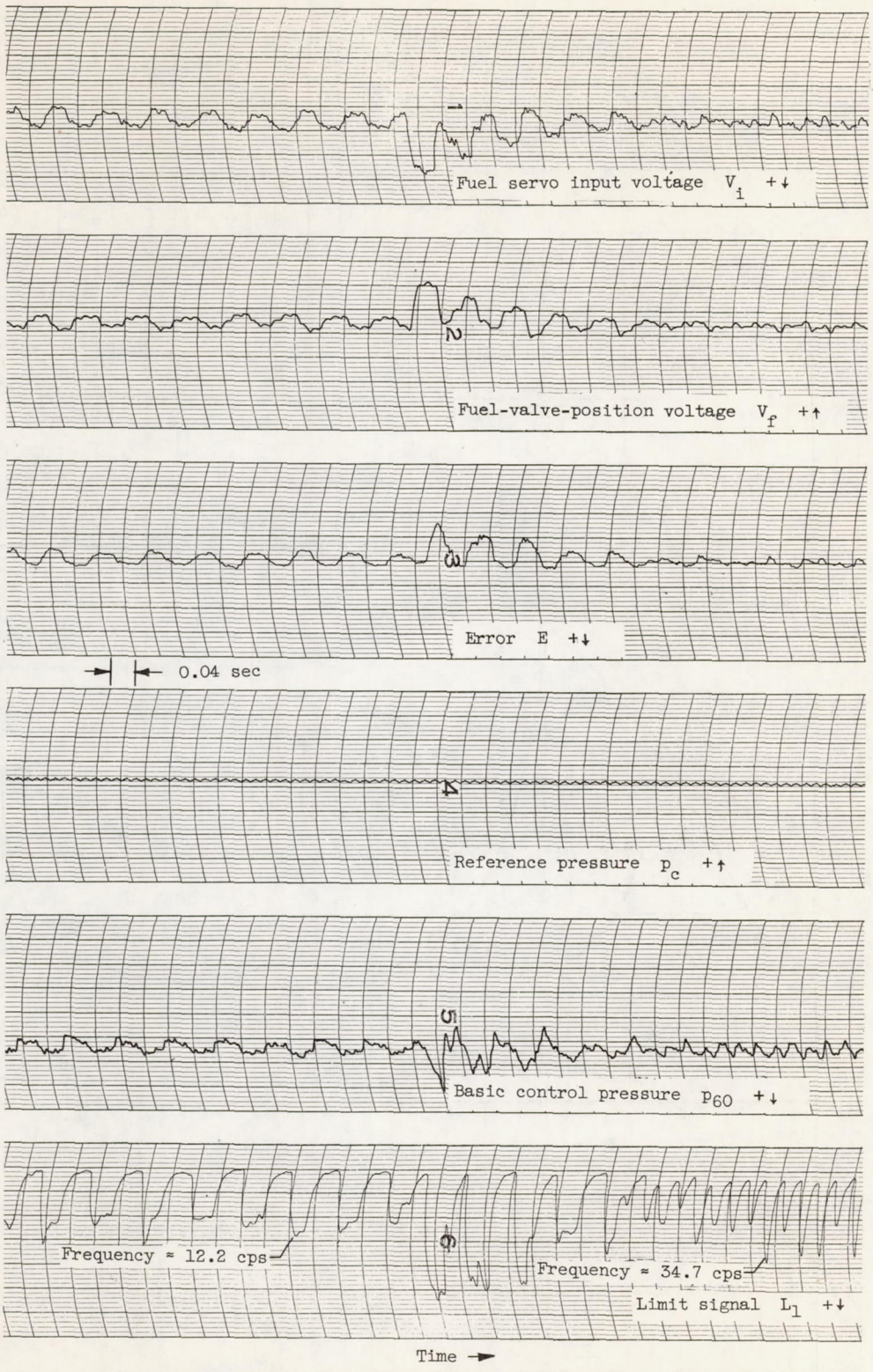

Figure 29. - Oscillogram of system instability at Mach 2.35.

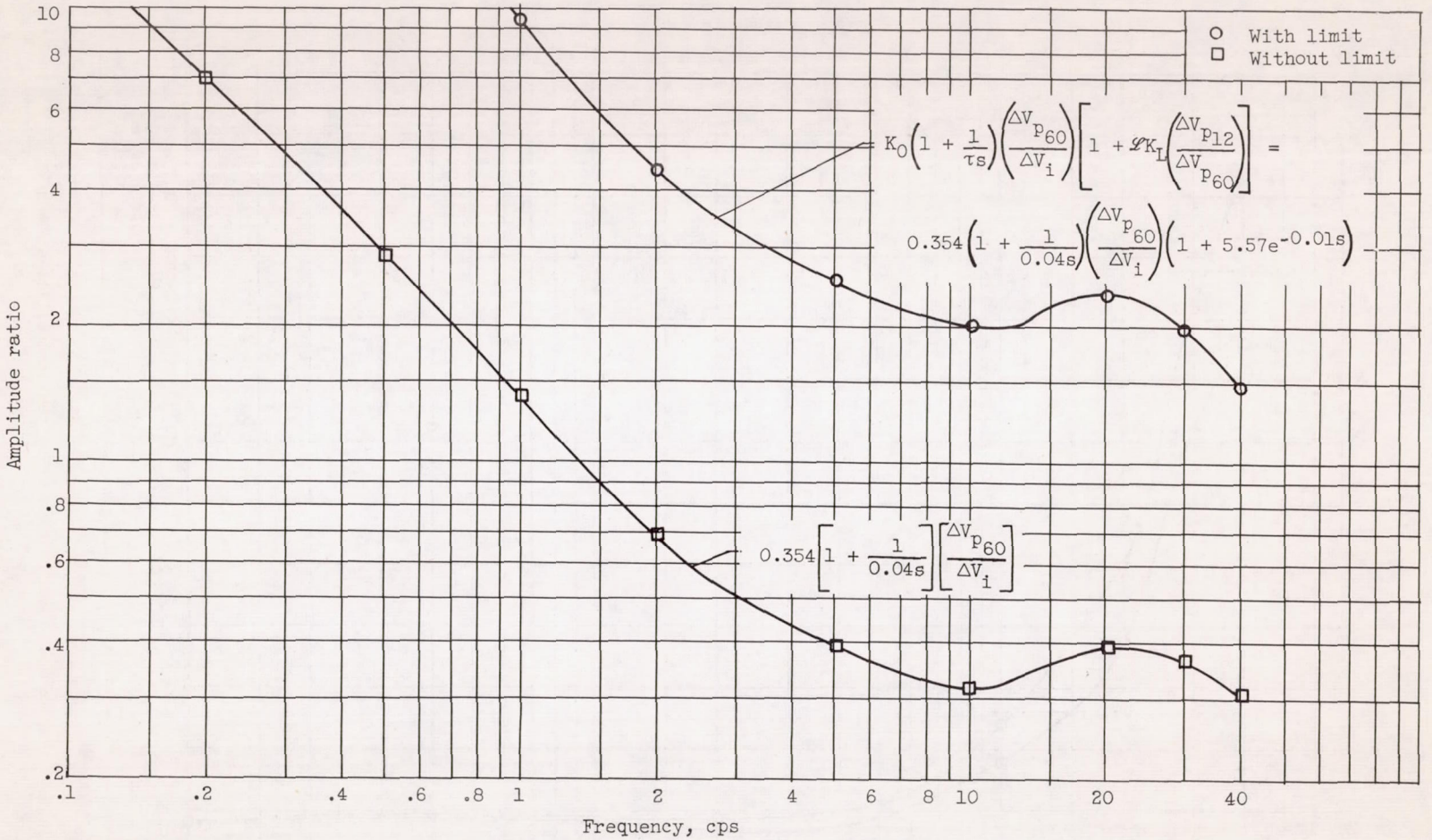

(a) Amplitude ratio.

Figure 30. - Open-loop frequency response of system with and without limit.

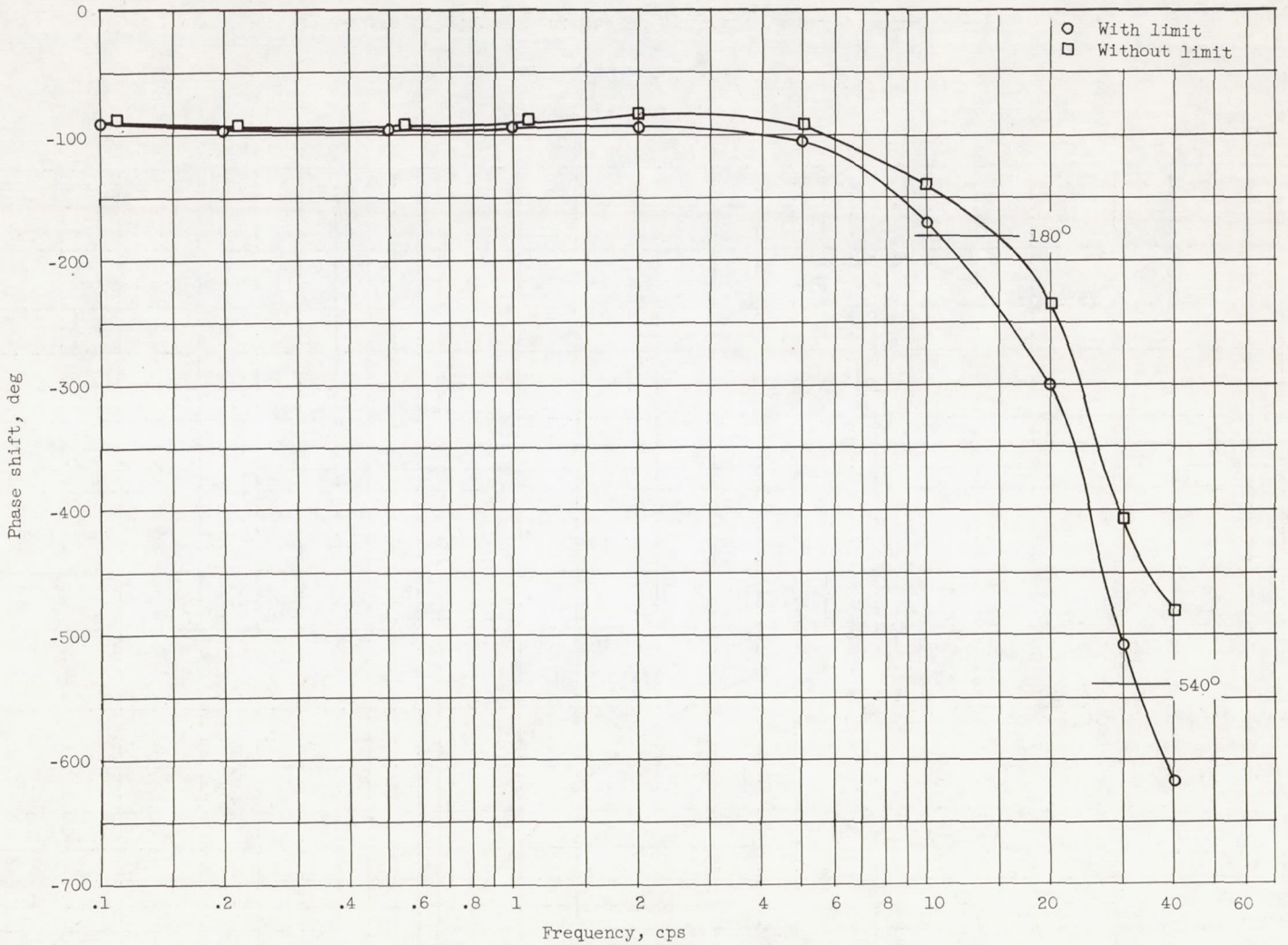

(b) Phase shift

Figure 30. - Concluded. Open-loop frequency response of system with and without limit.

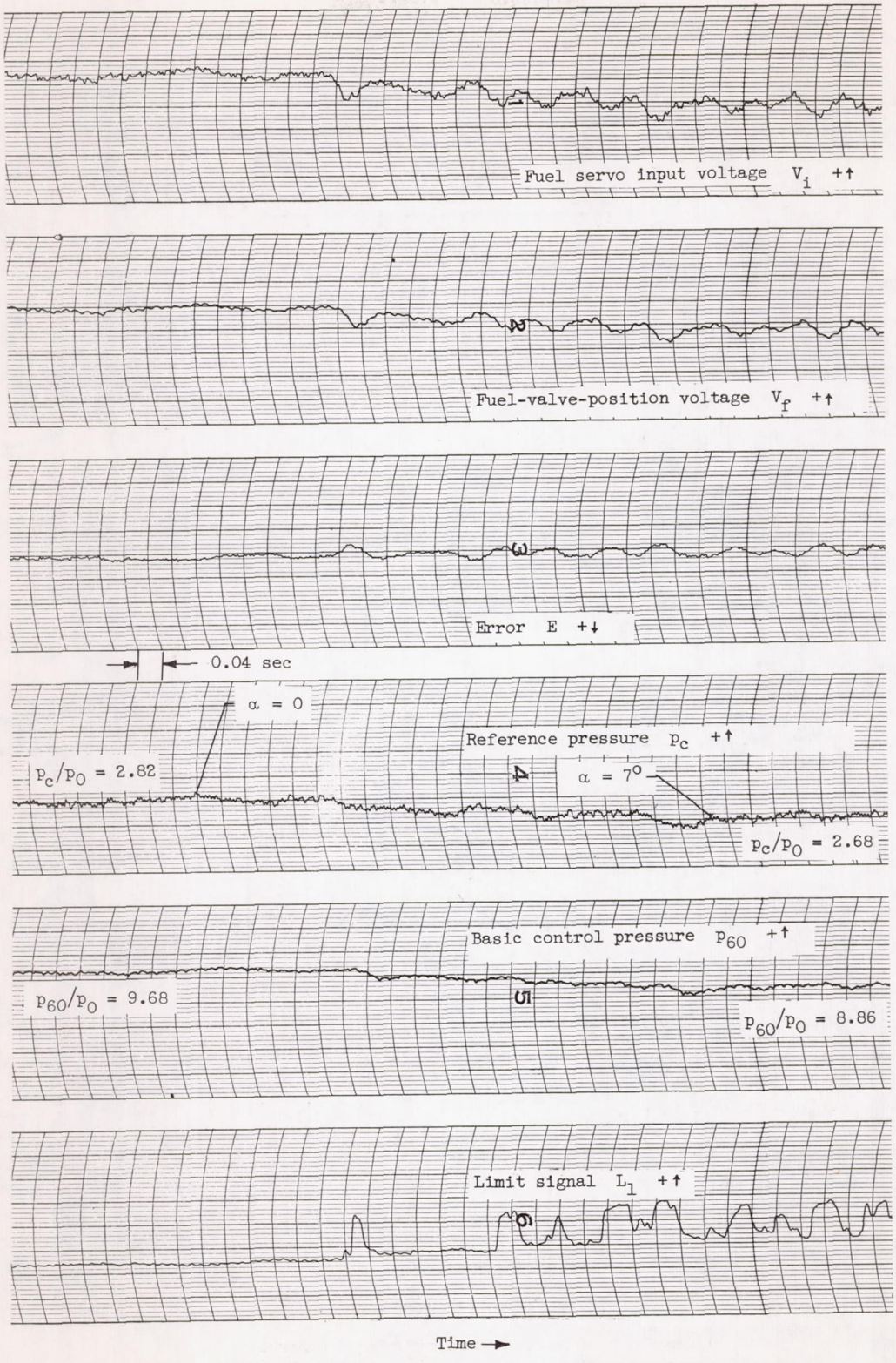

Figure 31. - Oscillogram of transient in angle of attack from zero to +7°.

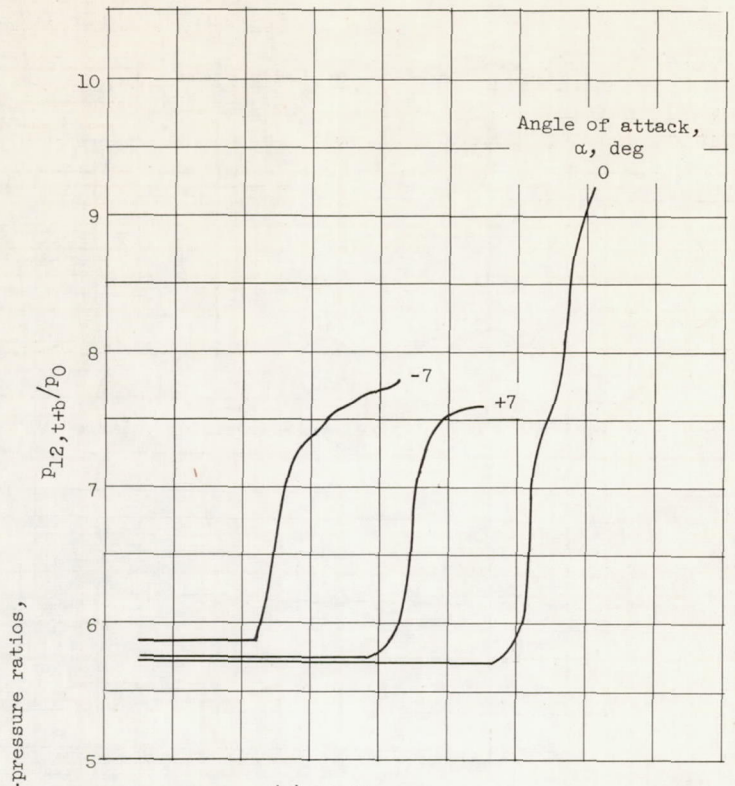

(a) Limit pressure.

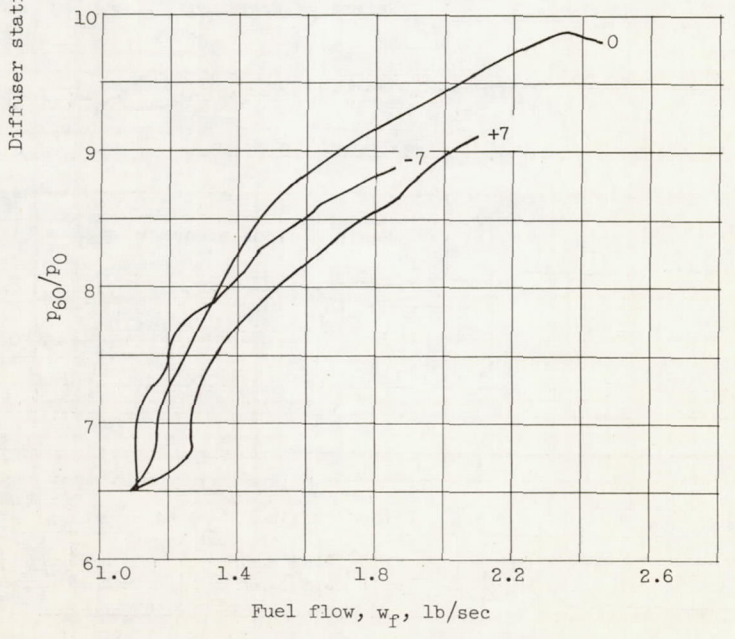

Diffuser static-pressure ratios,

(b) Basic control pressure.

Figure 32. - Angle-of-attack effects on control pressures. Mach number, 2.50; altitude, 60,000 feet.

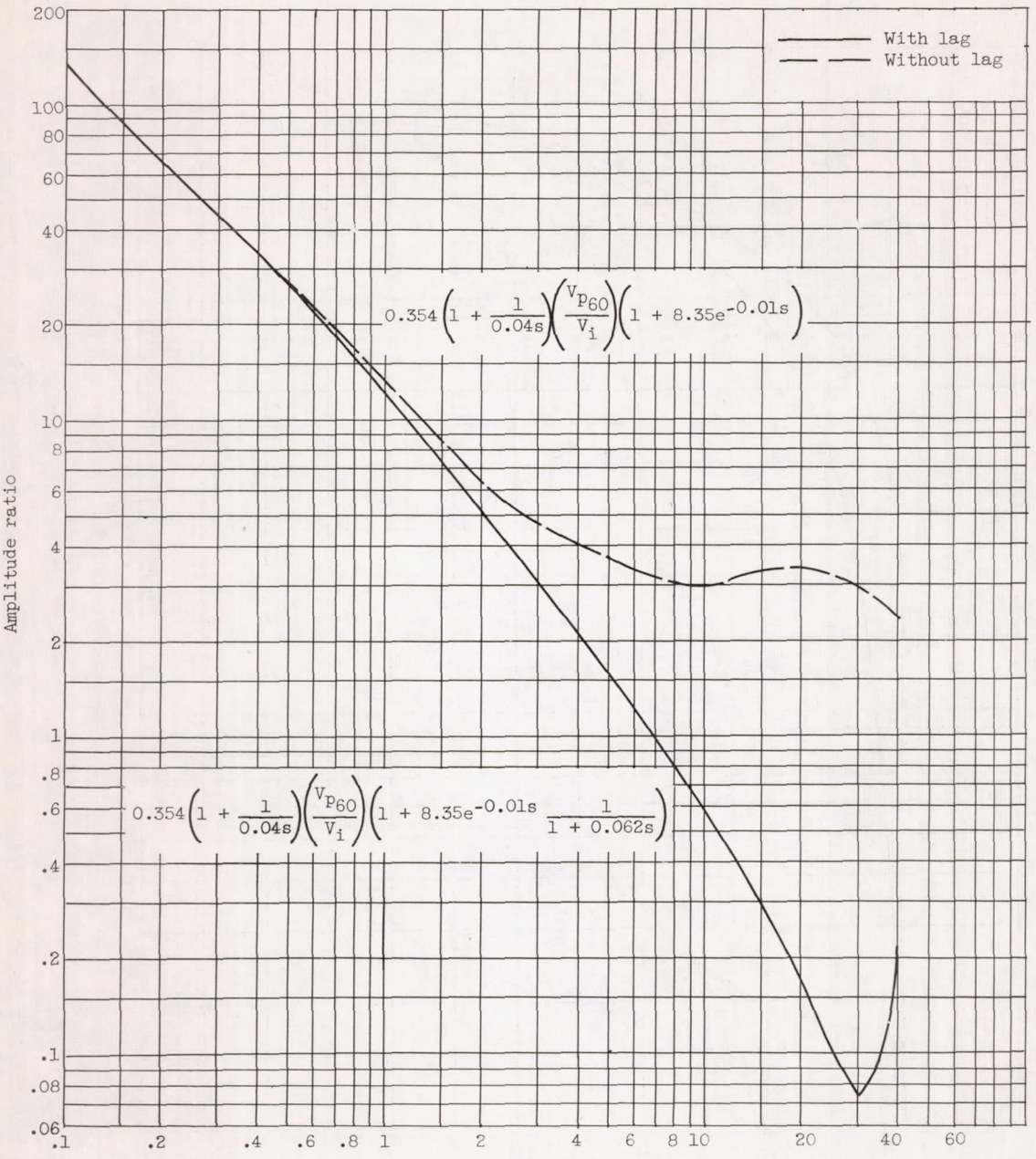

(a) Amplitude ratio.

Figure 33. - Stabilization of limit loop by addition of first-order lag.

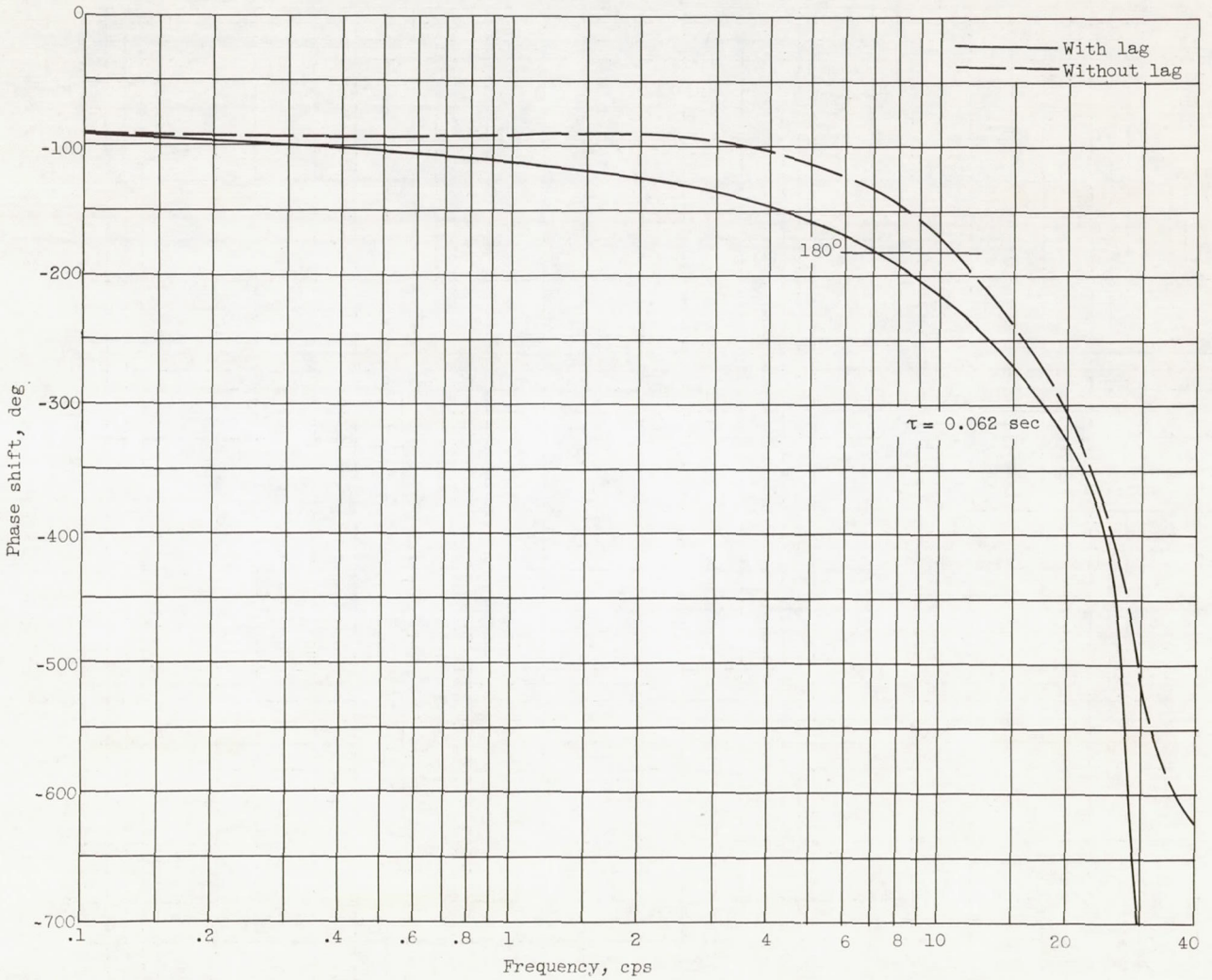

(b) Phase shift.

Figure 33. - Concluded. Stabilization of limit loop by addition of first-order lag.